Cellular and Molecular Gastroenterology and Hepatology

Activation of Intestinal Epithelial GABA A Receptors Ameliorates Alcohol-Related Liver Disease by Improving Intestinal Barrier Integrity

--Manuscript Draft--

Manuscript Number:	CMGH-D-25-01425
Full Title:	Activation of Intestinal Epithelial GABA A Receptors Ameliorates Alcohol-Related Liver Disease by Improving Intestinal Barrier Integrity
Article Type:	Original Research - Liver
Abstract:	Background & aims A central pathogenic mechanism in alcohol-related liver disease (ALD) involves a disruption of the gut barrier function and thus the bidirectional communication between the gut and liver, referred as the "gut-liver axis". While gamma-aminobutyric acid (GABA) and type A GABA receptors (GABAARs) are present in the intestinal epithelium, their role in the gut-liver axis and contribution to the pathogenesis of ALD, remains poorly understood. Methods A Gao-binge mouse model of ALD, as well as Gabra1IEC-KO mice and intestinal cell lines were employed as approaches to assess the role of GABAARs-mediated signaling in ethanol-induced liver injury. Results Administration of GABA markedly improved liver function and intestinal barrier integrity in ALD mice. This improvement was associated with a downregulation of intestinal cytochrome P450 2E1 (CYP2E1) expression and a reduction of oxidative stress. These beneficial effects of GABA on intestinal integrity and liver function were substantially diminished by the GABAAR antagonist, picrotoxin. In addition, picrotoxin blocked GABA's effect on CYP2E1 expression,, thereby preventing the attentuation of oxidative stress in the intestines of ALD mice. Moreover, when ethanol-stimulated cell models were subjected to pharmacological or genetic inhibition of CYP2E1, GABA treatment failed to produce any decrease in ROS levels. Finally, results from the intestinal epithelial-specific Gabra1 knockout mouse model demonstrated that the benifical effect of GABA on liver function in ALD is mediated by its activation of intestinal epithelial GABAARs. Remarkably, the pivotal role of intestinal CYP2E1 was robustly validated by confirming its dysregulated expression in patient-derived clinical samples. Conclusions Our results suggest that activation of intestinal GABAAR-mediated signaling reduces intestinal CYP2E1 expression and oxidative stress, thereby improving intestinal barrier function and alleviating ethanol-induced liver injury. Such findings suggest that intestinal GABA signaling offers a promising avenue for the development of novel strategies in the treatment of ALD.

Activation of Intestinal Epithelial $GABA_A$ Receptors Ameliorates Alcohol-Related Liver Disease by Improving Intestinal Barrier Integrity

Lushun Ma[1, 2, 5†], Tianxing Ren[1†], Haojie Zhang[1†], Xinyu Ge[2†], Wenshan Jiang[1], Yan Yu[1], Luoting Guo[1], Jingyi He[3], Bowen Liu[1], Liying Fang[1], Song Wang[2], Zinuo Zhang[1], Yuanhao Cui[1], Yunling Chen[1]; Chuanyong Liu[1, 4*], Shuanglian Wang[1*], and Daqing Sun[2*]

[1] Science and Technology Innovation Center, Shandong First Medical University, Jinan, China.

[2] Department of Pediatric Surgery, Tianjin Medical University General Hospital, Tianjin, China.

[3] Shandong Provincial Hospital Affiliated to Shandong First Medical University, Jinan, China.

[4] Department of Physiology and Pathophysiology, School of Basic Medical Science, Shandong University, Jinan, China.

[5] Department of Thyroid Surgery, Weifang People's Hospital, Shandong Second Medical University, Weifang, China.

†These authors contributed equally to this work.

*To whom correspondence should be addressed. Chuanyong Liu, e-mail: Liucy@sdu.edu.cn; Shuanglian Wang, e-mail: wsl6319@sdu.edu.cn; Daqing Sun, e-mail: sdqchris2019@tmu.edu.cn

Highlights

In alcohol-related liver disease, the intestinal $GABA_AR$-mediated signaling system is inhibited.

Activation of intestinal $GABA_ARs$ can enhance gut barrier function and ameliorate liver injury.

The therapeutic mechanism of $GABA_ARs$ in improving gut barrier function and

alleviating liver injury involves the modulation of CYP2E1 activity.

Abstract

Background & aims

A central pathogenic mechanism in alcohol-related liver disease (ALD) involves a disruption of the gut barrier function and thus the bidirectional communication between the gut and liver, referred as the "gut-liver axis". While gamma-aminobutyric acid (GABA) and type A GABA receptors ($GABA_AR$s) are present in the intestinal epithelium, their role in the gut-liver axis and contribution to the pathogenesis of ALD, remains poorly understood.

Methods

A Gao-binge mouse model of ALD, as well as *Gabra1*$^{IEC\text{-}KO}$ mice and intestinal cell lines were employed as approaches to assess the role of $GABA_AR$s-mediated signaling in ethanol-induced liver injury.

Results

Administration of GABA markedly improved liver function and intestinal barrier integrity in ALD mice. This improvement was associated with a downregulation of intestinal cytochrome P450 2E1 (CYP2E1) expression and a reduction of oxidative stress. These beneficial effects of GABA on intestinal integrity and liver function were substantially diminished by the $GABA_AR$ antagonist, picrotoxin. In addition, picrotoxin blocked GABA's effect on CYP2E1 expression,, thereby preventing the attentuation of oxidative stress in the intestines of ALD mice. Moreover, when ethanol-stimulated cell models were subjected to pharmacological or genetic inhibition of CYP2E1, GABA treatment failed to produce any decrease in ROS levels. Finally, results from the intestinal epithelial-specific *Gabra1* knockout mouse model demonstrated that the benifical effect of GABA on liver function in ALD is mediated by its activation of intestinal epithelial $GABA_AR$s. Remarkably, the pivotal role of intestinal CYP2E1 was robustly validated by confirming its dysregulated expression in patient-derived clinical samples.

Conclusions

Our results suggest that activation of intestinal $GABA_AR$-mediated signaling reduces intestinal CYP2E1 expression and oxidative stress, thereby improving intestinal barrier function and alleviating ethanol-induced liver injury. Such findings suggest that intestinal GABA signaling offers a promising avenue for the development of novel strategies in the treatment of ALD.

Graphical abstract

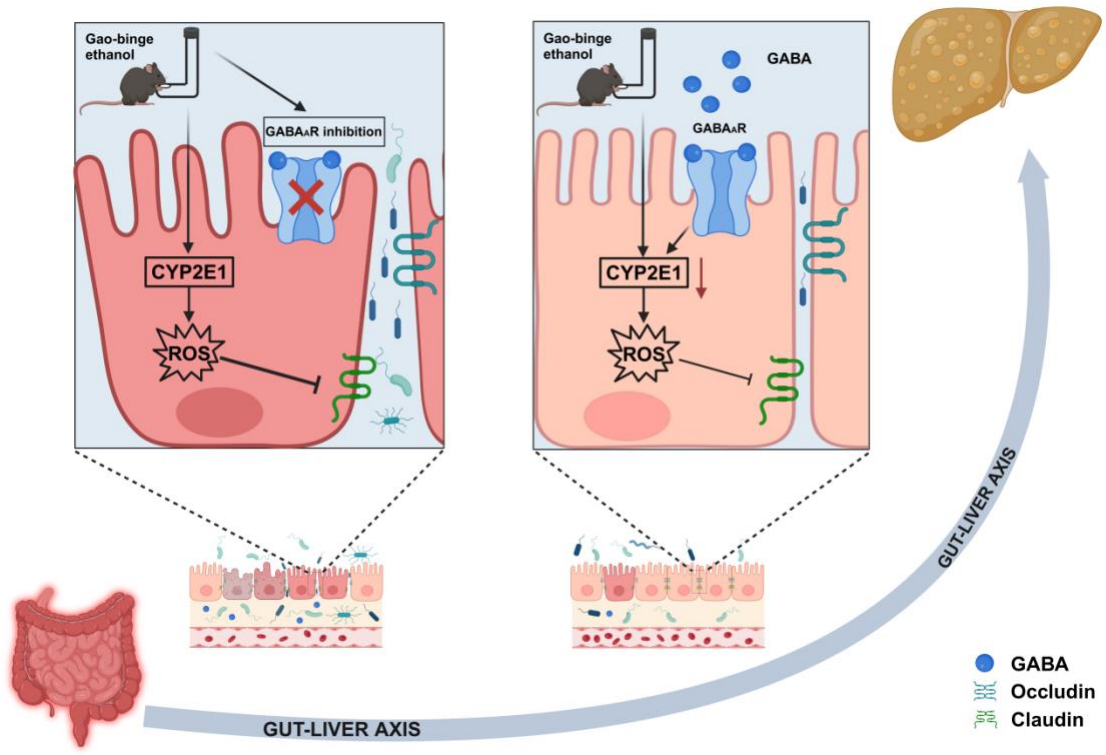

Keywords: alcohol-related liver disease, gut-liver axis, intestinal barrier, gamma-aminobutyric acid, cytochrome P450 2E1, oxidative stress

1. Introduction

Alcohol-related liver disease (ALD), a pathological condition arising from prolonged and excessive alcohol consumption, represents one of the leading causes of alcohol-related morbidity and mortality worldwide [1-4]. ALD encompasses a spectrum of diseases including hepatic steatosis, alcohol-related hepatitis, fibrosis, cirrhosis, and even hepatocellular carcinoma [5]. While the exact mechanisms underlying the pathogenesis and progression of ALD remain incompletely understood, results from

recent studies have highlighted a crucial role for the gut-liver axis in ALD pathogenesis [6].

The intestinal epithelium functions as a protective barrier through various mechanisms, including chemical defenses, physical integrity, and immune responses. Of note, chronic alcohol consumption disrupts this barrier, leading to gut microbiota imbalances (dysbiosis) [7-9]. As a result, harmful microbiota and their metabolites, such as lipopolysaccharides (LPS), breach the compromised barrier and enter the liver via the portal vein as pathogen-associated molecular patterns (PAMPs). This process triggers hepatic inflammation through the activation of Kupffer cells and interactions with the Toll-like receptor 4 (TLR4), thus contributing to the development and progression of ALD [10,11].

Recent studies have identified promising new approaches for the treatment of ALD which consist of targeting ethanol-induced intestinal barrier dysfunction as well as modification of gut-liver axis. For example, Song et. al [12] demonstrated that Pomegranate can reduce intestinal oxidative stress in ALD mice and enhance tight junction protein expression, thereby improving liver function. Moreover, supplementation with Red raspberry and the gut microbiota metabolite Propionate has been demonstrated to exert therapeutic effects in ALD mice by improving intestinal barrier function and modulating gut microbiota composition [13,14]. Remarkably, recent studies conducted in alcohol-associated hepatitis patients have demonstrated that novel therapies targeting the dysfunctional gut-liver axis-such as fecal microbiota transplantation (FMT)[1], probiotics[2] and bacterio-phages[3] exhibit potential benefits in ALD treatment. Despite these advances, the precise mechanisms through which ethanol impairs intestinal barrier function and gut-liver axis in ALD remain incompletely elucidated. This problem is further compounded by the lack of any FDA-approved pharmacological agents specifically designed to restore intestinal barrier function. Therefore, developing targeted pharmacological strategies to restore intestinal barrier integrity and improve liver function represents a significant endeavor for the development of novel therapeutic approaches for ALD.

Gamma-aminobutyric acid (GABA) is the principal inhibitory neurotransmitter in the central nervous system [15]. It is synthesized from glutamate by glutamate decarboxylase (GAD) [16] and exerts its biological effects via type A or B receptors ($GABA_ARs$ or $GABA_BRs$) [17]. Recent findings have revealed the presence of the GABA signaling system in peripheral tissues, including the intestine, where it has been implicated in gastrointestinal disorders such as allergic diarrhea and chemoradiotherapy-related side effects [18,19]. Given that $GABA_AR$ is a primary target for ethanol in the central nervous system and is involved in ethanol-associated neural conditions [20,21], we hypothesized that the $GABA_ARs$-mediated signaling system in intestinal epithelial cells may also contribute to ethanol-induced disruptions in intestinal permeability. Therefore, in the present study, experiments were designed to test this hypothesis and further assess whether this $GABA_ARs$-mediated pathway affects the ALD phenotype via the gut-liver axis.

2.Materials and methods

2.1 Human colon biopsies

Human colon tissues were obtained from 6 male patients between the ages of 55 and 60 years, who had undergone a partial colectomy in the Shandong Provincial Hospital. Participants were categorized according to their history of alcohol consumption. The case group was composed of 3 individuals with a documented history of sustained heavy alcohol intake (≥ 5 years). Healthy control group comprised 3 age-matched individuals with no history of alcohol consumption. Written informed consent was obtained from each subject prior to enrollment in the study. The procedures were approved by the Ethics Committee of the Shandong Provincial Hospital.

2.1 Animal models

The study was conducted according to the guidelines of the Declaration of Helsinki. All animal experiments were performed in accordance with National Institutes of Health

guide for the care and use of laboratory animals. Male C57BL/6J mice (6-8 weeks old, 20 – 25 g) were purchased from Vital River Laboratories (Beijing, China) and housed at 24°C with a 12 h light/dark cycle and 50 ± 5% relative humidity. All mice were acclimated to these conditions for a minimum of 5 days prior to use in the experiments. The mouse model of chronic-plus-binge alcohol feeding (hereafter referred to as the Gao-binge ALD model) has been described previously and shown to be effective in inducing steatosis, liver injury and inflammation in these mice [22]. Briefly, mice were divided randomly into two groups. The ethanol-fed mice were subjected to a 5-day adaptation period with Lieber-DeCarli liquid diet, followed by 10 days of feeding with a 5% alcohol-containing Lieber-DeCarli liquid diet (710260, Dyets, USA) [23]. The pair-fed control mice received an isocaloric control liquid diet (710027, Dyets, USA). On the final day of feeding (day 16), ethanol- and pair-fed mice were gavaged with ethanol (5 g/kg) or maltose dextran (9 g/kg), respectively, and euthanized at 9 h post-gavage. For treatments involving $GABA_AR$-related drugs, mice were injected daily with GABA (i.p. 200 mg/kg, A5835-25G, Sigma, USA)[4, 5] or every two days with the GABAAR antagonist, picrotoxin (PTXN, i.p. 2 mg/kg, HY-101391, MCE, USA)[5], starting from day 6 of their alcohol/control treatments (Figure 1A).

Intestine-specific *Gabra1* knockout and control mice were generated by administering AAV9-villin-Cre virus or AAV9-villin-NC virus (GeneChem, Shanghai, CHN), respectively, to $Gabra1^{flox/flox}$ mice (Provided by Dr. Jinxin Li at Shandong University). At 3 weeks post-AAV injection, the Gao-binge model was established, and mice were treated daily with GABA (i.p. 200 mg/kg). The above-mentioned mice were sacrificed as described, blood and tissue samples were collected for further experiments. All animal procedures were approved by the Ethics Committee for Animal Experiments of Shandong First Medical University & Shandong Academy of Medical Sciences (Approval No. W202410120164).

2.2 Cell culture and treatments

The human normal colonic epithelial CCD841 cell line was purchased from the

Cellverse (iCell) Bioscience Technology Co., Ltd (Shanghai，CHN) and cultured in Dulbecco's Modified Eagle High Glucose Medium (KGM12800N, KeyGEN, CHN) supplemented with 10% fetal bovine serum (SE141, SeraPure, GER) and 1% Penicillin-Streptomycin (C55-SV30010, Canspec, CHN). The human colonic carcinoma T84 cell line was purchased from Cyagen Biosciences Inc (Suzhou，CHN) and cultured in Dulbecco's Modified Eagle F12 Medium (KGM12500N, KeyGEN, CHN) supplemented with 10% fetal bovine serum and 1% Penicillin-Streptomycin. Cells were maintained in a humidified incubator with 5% CO_2 at 37℃. Small interfering RNA (siRNA) targeting CYP2E1 were purchased from RiboBio Co., Ltd (Guangzhou, CHN) and transfected into cells using INTERFERin (10100036, Polyplus, FRA). Twenty-four hours post-transfection, cells were treated with ethanol for 48 h and harvested for further analysis.

For ethanol treatments, cells were cultured with medium containing 100 mM ethanol for 48 h. The culture dishes were sealed with laboratory film throughout the treatment period to minimize ethanol evaporation. The medium was refreshed every 12 h. For $GABA_AR$-specific agonist treatment, muscimol (HY-N2313, MCE, USA) was added to the medium at a final concentration of 100 μM and incubated for 48 h at 37 ℃. To achieve a pharmacological inhibition of $GABA_AR$, cells were co-incubated with 100 μM of the non-competitive antagonist, picrotoxin (PTXN), in the presence of ethanol stimulation. A pharmacological inhibition of CYP2E1 in intestinal epithelial cells was achieved by co-incubating cells with 50 μM Clomethiazole (533-45-9, Proteintech, CHN) for 48 h at 37 ℃, during the ethanol treatment.

2.3 Detection of ROS in colonic epithelial cells

Cells were cultured in confocal dishes and exposed to ethanol for 48 h, followed by treatment with GABA (50 μM). The DEFC-DA probe (S0033S, Beyotime, CHN) was mixed with Hoechst nuclear staining solution (C1011, Beyotime, CHN) in serum-free medium and incubated with the cells at 37°C for 20 min in a CO_2 incubator. Subsequently, cells were washed 3 times with PBS. ROS production was then observed using a confocal microscope (Celldiscoverer7, ZEISS, GER).

2.4 Serum alanine aminotransferase, malondialdehyde and lipopolysaccharide, and hepatic triglyceride analyses

Whole blood samples from the mice were incubated at room temperature for 30 min, followed by centrifugation at 3000 rpm for 20 min to obtain serum. Serum levels of alanine aminotransferase (ALT) were determined according to the manufacturer's protocols (C009-2-1, Njjcbio, CHN). Malondialdehyde (MDA) content in fresh liver tissues was assayed using the thiobarbituric acid method (A003-2, Njjcbio, CHN). Portal venous and hepatic Lipopolysaccharide (LPS) concentrations were quantified with a commercial murine LPS enzyme-linked immunosorbent assay (ELISA) kit (CSB-E13066m, Cusabio, CHN) following the manufacturer's protocol. Hepatic triglyceride (TG) levels were measured according to the manufacturer's protocols (A110-1-1, Njjcbio, CHN).

2.5 Colon and liver histopathology

Colon and liver tissues were fixed in 4% paraformaldehyde solution (BL539A, Biosharp, CHN), followed by incubation in 30% sucrose solution at 4℃ overnight. Tissues were then embedded in paraffin, sectioned into 5 μm thick slices and stained using hematoxylin (G1080, Solarbio, CHN) and eosin (G1100, Solarbio, CHN) or alcian blue (G1560, Solarbio, CHN). For immunohistochemical staining, antigen retrieval from colon sections was conducted by boiling dewaxed slices in citrate buffer (pH 6.0, C1032, Solarbio, CHN). Then, endogenous peroxidase activity in the tissue was blocked according to the protocols provided by the manufactures (PV-9000, Zsbio, CHN). Tissues were incubated at 4℃ overnight with primary antibodies aganist CYP2E1 (Abcam, ab28146) or 8-OHdG (Santa Cruz, sc-66036), followed by incubation with horseradish peroxidase-conjugated secondary antibodies (Abcam, ab150080). Subsequently, the tissues were sequentially incubated with Diaminobenzidine chromogen (ZLI-9017, Zsbio, CHN) and counterstained with Hematoxylin, followed by imaging under an optical microscope (ML31, Mshot, CHN). For Oil Red O staining, frozen liver tissues were embedded in optimal cutting

temperature compound (4583, SAKURA, JPN) and sectioned into 5 μm cryosections using a cryostat (Thermofisher CryoStar NX70, USA). Oil Red O staining was then performed according to the manufacturer's protocol. (C0158M, Beyotime, CHN). For transmission electron microscopy, gut tissue sections were dissected into small pieces as required and immersed in a fixative solution. Transmission electron microscopic images were captured using a transmission electron microscope (HT7800, Hitachi High-Tech, JPN) by investigators who were blinded to the experimental conditions of the samples.

2.6 Detection of colonic mucins

Colonic mucin secretion was evaluated using an Alcian Blue staining kit (G1560, Solarbio, CHN) on paraffin-embedded tissue sections. Initially, sections were immersed in an acidic solution for 3 min, then transferred to an Alcian Blue staining solution and incubated at room temperature in the dark for 30 min, followed by washing with tap water. Subsequently, the sections were stained with nuclear fast red for 5 min and rinsed again with tap water. Finally, the tissue sections were dehydrated through a graded ethanol series, cleared with xylene, and mounted in neutral resin.

2.7 Intestinal microbiota cultivation

Equal portions of freshly prepared liver tissue were weighed and homogenized in sterile PBS. Aliquots of the homogenate were then plated onto the Demand-Rogosa-Sharpe culture medium (M8330, Solarbio, CHN) incubated for 36 h at 37°C. Colony formation was subsequently assessed to determine the *Lactobacilli* content in the liver tissue of the mice.

2.8 Colonic Organoid Culture

Distal colon tissues from wild-type (WT) mice were longitudinally opened, rinsed with ice-cold DPBS, and cut into 2-3 mm^3 fragments, followed by repeated washing in cold DPBS. Crypt isolation was performed by incubating the tissue fragments with 2 mM

EDTA (Invitrogen, USA) at 4 ℃ for 1 h with gentle shaking. After incubation, the crypts were collected by centrifugation at 300 × g for 5 min at 4 °C and quantified microscopically. Approximately 150 crypts were resuspended in 50 μL of Matrigel (Corning Inc, USA) and seeded into 48-well plates. Following Matrigel solidification, 250 μL of mouse colonic organoid medium (bioGenous BIOTECH, Inc. China) was added to each well. Organoids were cultured at 37 °C in a humidified atmosphere containing 5% CO_2 for 3 days, followed by stimulation with 50 mM ethanol for 12 h prior to immunofluorescence staining.

2.9 Gut permeability assays

After fasting for 6 h, mice were orally administered of FITC-dextran solution (400 mg/kg, 46944, Sigma, USA) to assess gut permeability. Blood samples were collected at 4 h post-administration and centrifuged at 2000 g for 10 min to separate the upper layer of serum. Fluorescent measurements were conducted using a fluorescent microplate reader (357-711186, Thermofisher, USA) with an emission of 530 nm and an excitation of 485 nm. Gut permeability was evaluated by quantifying the fluorescent intensities by investigators who were blinded to the experimental conditions of the samples.

2.10 RNA extraction, RT-PCR, and RT-qPCR

Total RNA was extracted from mouse liver and colon tissues or cultured cells using TRIzol reagent (CW0580S, CWBIO, CHN), and then converted into cDNA using a RNA reverse transcription kit (R223-01, Vazyme, CHN). Reverse transcription polymerase chain reaction (RT-PCR) was performed in a Thermo Fisher PCR thermal cycler using specific primers (sequences listed in Table S1). The amplification products were subjected to horizontal agarose gel electrophoresis and visualized using a gel imaging analysis system (BG-520, Baygene, CHN). Real-time quantitative polymerase chain reaction (RT-qPCR) was performed using a real-time fluorescent quantitative PCR instrument (Gentier 96R, TIANLONG, CHN) and a SYBR Green Premix Pro Taq HS qPCR Kit (CW0957, CWBIO, CHN). Relative gene expression was calculated

using the $-2^{\Delta\Delta Ct}$ method with *18S RNA* serving as the housekeeping gene. Primer sequences used in this study are presented in Table S2.

2.11 Western blotting

Mouse colon tissue and cultured cells were lysed using RIPA lysis buffer (G2002, Servicebio, CHN). Total protein extracts were quantified with use of a BCA protein assay kit (ZJ102, Epizyme, CHN). Subsequently, 25 - 30 μg of total protein was separated by 10% - 12% SDS-PAGE electrophoresis and transferred onto a 0.45 μm PVDF membrane (IEVH85R, Millipore, USA). The membrane was blocked with 5% non-fat milk for 2 h at room temperature, followed by overnight incubation at 4° C with primary antibodies: β-actin (Abcam, ab8227), Occludin (Invitrogen, 33-1500), Claudin 1 (Proteintech, 13050-1-AP), Claudin 4 (Proteintech, 16195-1-AP), CYP2E1 (Abcam, ab28146), 8-OHdG (Santa cruz, sc-66036), iNOS (Abcam, ab15323), 3-NT (Abcam, ab61392), 4-HNE (Abcam, ab46545), GABARAP (CST, 13733), GABARAPL1 (CST, 26632), GABARAPL2 (CST, 14256). Membranes were then washed with TBS-T and incubated with HRP-conjugated anti-mouse antibody (Proteintech, SA00001-1) or anti-rabbit antibody (Proteintech, SA00001-2) for 1 h at room temperature. Protein bands were visualized using an ECL chemiluminescent substrate (E422-02, Vazyme, CHN) and detected with a chemiluminescence imaging system (5200 Multi, Tanon, CHN). Western blot band densitometry was quantified using ImageJ software (National Institutes of Health, USA). Each experiment was performed in triplicate.

2.12 Immunofluorescent staining

Paraffin-embedded tissue sections were deparaffinized, rehydrated, and subjected to antigen retrieval by boiling in citrate buffer for 30 min. Sections were incubated with 0.2% Triton-X 100 for 30 min at room temperature, followed by blocking with 5% goat serum for 30 min. Primary antibodies, appropriately diluted, were applied and incubated at 4℃ overnight. Sections were washed 3 times with PBS and then incubated with fluorescent-conjugated secondary antibodies at 37℃ for 1 h. Finally, tissue

sections were mounted with a DAPI-containing mounting medium (S36968, Thermofisher, USA). The primary antibodies used were Occludin (Invitrogen, 33-1500) and MUC2 (Abcam, ab272692). The fluorescent secondary antibodies used were Goat Anti-Rabbit IgG H&L (Alexa Fluor® 594) (Abcam, ab150080) and Goat Anti-Mouse IgG H&L (Alexa Fluor® 488) (Abcam, ab150117). Fluorescent images of the samples were captured using a laser scanning confocal microscope (Celldiscoverer7, ZEISS, CER), and fluorescent quantification was performed using ImageJ software (National Institutes of Health, USA) by investigators who were blinded to the experimental conditions of the samples.

2.13 Statistical analysis

All data analysis and processing were performed using GraphPad Prism 9 software (GraphPad Software, USA), with data presented as Means ± SEMs. One-way analysis of variance (ANOVA) followed by post-hoc tests was utilized for comparisons among multiple groups A P value of < 0.05 were considered as statistically significant.

3 Results

3.1 Hepatoprotective effects of GABA in ALD mice

There were no statistically significant differences in food intake or body weight (**Supplemental Figure 1**) among the different groups (Control, EtOH, EtOH + GABA, and GABA alone) during the modeling phase. However, mice in the ethanol-treated (EtOH) group exhibited a significant increase in their liver-to-body weight ratios (liver index) (**Figure 1B**), serum ALT levels (**Figure 1C**), and portal venous LPS levels (**Figure 1D**), effects which were markedly reduced with GABA treatment. Results from our H&E staining of mouse liver tissues revealed substantial improvements in ALD pathology in response to GABA treatment. Specifically, there were reductions in lipid vacuolation and increased amounts of regular hepatic cord structure (**Figure 1H**), and significant reductions in alcohol-induced hepatic lipid accumulation were present, as based on Oil Red O staining (**Figure 1I**) and serum TG quantification (**Figure 1E**).

Moreover, hepatic lipid peroxidation levels were reduced with GABA treatment (**Figure 1F**) and, while alcohol-fed mice exhibited markedly increased hepatic mRNA expressions of pro-inflammatory cytokines (IL-1β, IL-6, and TNF-α) compared to controls, these increases were mitigated by GABA treatment (**Figure 1G**). Notably, GABA administration did not affect liver function in control mice (**Figures 1B-I**).

3.2 Protective effects of GABA on intestinal barrier function in ALD mice

Excessive ethanol intake severely disrupts intestinal barrier integrity, which promotes bacterial translocation and portal endotoxemia, thereby driving the progression of ALD [24]. To investigate whether the beneficial effects of GABA on ethanol-induced liver injury involved modulation of intestinal barrier function, we examined its influence on the gut phenotype in ALD mice. Histopathological analysis using H&E staining demonstrated a pronounced submucosal infiltration of inflammatory cells in the intestines of the EtOH-fed group **(Figure 2A)**. In contrast, ALD mice treated with GABA (EtOH + GABA group) exhibited a notable alleviation of this intestinal inflammation as compared to the EtOH group. Given the abundance of *lactobacilli* in mammalian intestines, we cultured liver homogenates in *lactobacillus*-specific media [25] and found that, while a significant increase in intestinal dysbiosis was present in the livers of ALD, these increases were substantially mitigated by GABA treatment (**Figure 2B**).

Intestinal permeability was further assessed using FITC-dextran gavage and serum fluorescent quantification. Mice in the EtOH + GABA group exhibited significantly lower serum FITC-dextran fluorescence compared to those in the EtOH group (**Figure 2C**), .and 16S rRNA expression levels in the livers of the EtOH + GABA group mice were significantly reduced (**Figure 2D**). Transmission electron microscopy provided further insights into intestinal barrier function and revealed an improvement in tight junction integrity within GABA-treated ALD mice as compared to the EtOH group (**Figure 2E**). In line with these findings, our immunofluorescent and Western blot analyses demonstrated an upregulation in the protein levels of Occludin, Claudin-1, and Claudin-4 in the intestines of the EtOH + GABA group mice versus EtOH group (**Figures 2F-G**). Moreover, GABA treatment was associated with an increase in

intestinal mucous secretions, as demonstrated by Alcian Blue and MUC2 staining (**Figures 2H-I**).

3.3 Downregulation of intestinal CYP2E1 expression and reduction of oxidative stress levels in ALD mice by GABA treatment

Alcohol-induced impairment of intestinal barrier function has been reported to be linked to increased expression of CYP2E1 and oxidative stress [26,27]. Of note, accumulating evidence indicates that the underlying mechanism for GABA's cytoprotective action involves its potent antioxidant properties[6, 7]. As based on these reports, we thus hypothesized that GABA may improve intestinal barrier function in ALD mice by modulating CYP2E1 expression at this site. Of note, immunofluorescence staining analysis revealed a marked upregulation of intestinal CYP2E1 expression in individuals with chronic alcohol consumption compared to age-matched healthy controls (**Figures 3A**). Consistent with observations in human samples, immunofluorescence analysis demonstrates that ethanol stimulation upregulates CYP2E1 expression in ex vivo cultured mouse colon organoids (**Figures 3B**). Results from Western blot (**Figures 3C**) and immunohistochemical (**Figures 3D**) analyses revealed a significant increase in intestinal CYP2E1 protein levels in ALD mice, an effect which was restored by GABA treatment. Additionally, levels OHdG, a biomarker of oxidative DNA damage [28], were markedly reduced in the intestines of ALD mice following GABA treatment (**Figures 3E**). Moreover, Western blot results also showed elevated levels of oxidative stress markers such as 4-HNE, 3-NT, and iNOS, as observed within the intestines of ALD mice, were significantly mitigated by GABA treatment (**Figures 3F-G**).

3.4 $GABA_AR$ modulation of intestinal barrier function in ALD mice

Building upon previous research which underscored the critical role for $GABA_AR$-mediated signaling pathways in response to ethanol-induced stimuli within the central nervous system [29,30], we assessed the expression of $GABA_AR$ subunits in the colon of ALD mice. Results from RT-qPCR analysis revealed the expression of 15 $GABA_AR$ subunits, wherein ethanol exposure resulted in significant reductions in mRNA levels of the *Gabra1, Gabra5, Gabra6, Gabrb1*, and *Gabrr3* subunits, while *Gabra3* and

Gabrd mRNA levels were significantly elevated (**Figure 4A**). In line with this transcriptional pattern, immunofluorescence analysis further verified that ex vivo ethanol stimulation downregulates GABRA1 protein expression in mouse colon organoids(**Figure 4B**). Concurrently, elevated levels of GABA and its synthetic enzyme GAD65 were detected in colonic tissues of ALD model mice(**Figure 4C**).

To further examine the role of intestinal $GABA_AR$s in ethanol-induced liver injury, we conducted a second set of experiments with the following groups: control, EtOH, EtOH + GABA, EtOH + GABA + PTXN, and EtOH + PTXN. Of note, mice in the EtOH + GABA + PTXN group exhibited a significant increase in their liver index (**Supplemental Figure 4A**) and serum ALT levels (**Figure 4D**) compared to that obtained in the EtOH + GABA group, indicating that $GABA_AR$ inhibition restricted the beneficial effects of GABA on liver function. Histopathological examinations using H&E (**Figure 4E**) and Oil Red O (**Figure 4F**) staining revealed an increased number of lipid vacuoles in the livers of mice from the EtOH + GABA + PTXN group, suggesting the presence of an exacerbated degree of hepatic steatosis compared to that in the EtOH + GABA group. The role of intestinal $GABA_AR$s upon intestinal permeability was also investigated within ALD mice. Culturing liver homogenates in *lactobacillus* media revealed that significantly greater numbers of colonies were formed in the EtOH + GABA + PTXN compared to the EtOH + GABA group (**Supplemental Figure 4B**). FITC-dextran fluorescent intensity analysis from blood samples confirmed that PTXN intervention impaired the protective effects of GABA on intestinal barrier integrity in ALD mice (**Supplemental Figure 4C**). In accord with these functional assay results, transmission electron microscopy revealed decreased levels of compacted tight junction proteins in the intestinal epithelium of the EtOH + GABA + PTXN versus EtOH + GABA group (**Figure 4G**). Western blot analyses (**Figures 4H**) and immunofluorescence staining (**Figures 4I**) provide further evidence demonstrating that PTXN treatment blunted the GABA-induced increases in intestinal protein levels of Occludin, Claudin-1, and Claudin-4. Interestingly, intestinal barrier function in ALD mice treated with PTXN alone (EtOH + PTXN group) did not show any further deterioration. Collectively, these findings provide strong support indicating that

GABA's protective effects on intestinal barrier function in ALD mice are mediated through $GABA_AR$ signaling pathways.

3.5 Activation of intestinal $GABA_ARs$ downregulates CYP2E1 expression and alleviates oxidative stress in ALD mice

We next sought to investigate whether GABA-$GABA_ARs$ modulates intestinal barrier function by downregulating CYP2E1. With use of Western blot, we found that mice in the EtOH + GABA + PTXN group exhibited significantly increased expression levels of intestinal CYP2E1 as compared with that observed in the EtOH + GABA group (**Figures 5B**). Consistent with this result, immunohistochemistry results demonstrated that PTXN attenuated the GABA-induced downregulation of intestinal CYP2E1 (**Figures 5A**) and, within mouse colon tissue there were increased levels of 8-OHdG in the EtOH + GABA + PTXN versus EtOH + GABA group (**Figures 5C**). Moreover, intestinal iNOS and 3-NT levels were also found to be significantly higher in the EtOH + GABA + PTXN compared to the EtOH + GABA group (**Figures 5D**).

We next explored some of the mechanism by which $GABA_ARs$ upregulate CYP2E1 protein levels. GABA type A receptor-associated protein (GABARAP) is known for regulating the trafficking of $GABA_AR$ to cell membranes and is implicated in various $GABA_AR$-related pathophysiological mechanisms [31]. For example, GABARAP has been reported to influence protein stability through ubiquitination modification [32]. With our Western blots we found that elevated GABARAPL2 expressions were present in the colon of mice from the EtOH group. This effect was reversed by GABA treatment, while no significant changes were observed in GABARAP and GABARAPL1 (**Supplemental Figure 5A**). These results suggest that $GABA_AR$ may modulate intestinal CYP2E1 expression through GABARAPL2.

3.6 Activation of intestinal $GABA_ARs$ enhances tight junction proteins and downregulates CYP2E1 protein expressions

As an approach to further validate the role of CYP2E1 in the upregulation of barrier proteins by $GABA_ARs$, we used the CCD841 and T84 human colon epithelial cell lines, which express several $GABA_AR$ subunits (**Figure 6A**). Based on our CCK-8 assay results (**Figures 6B and 6C**), a 50 μM concentration of GABA was selected for

subsequent experiments. Our Western blot analysis revealed that alcohol treatment (100 mM) reduced the expression of Occludin, Claudin1, and Claudin4 in both CCD841 (**Figures 6D**) and T84 (**Figures 6E**) cells. Notably, similar to the effects of GABA, the selective $GABA_AR$ agonist, muscimol (MUS), upregulated the expression of these tight junction proteins in both cell types, providing robust support for an involvement of $GABA_ARs$ in regulating tight junction protein expression. Consistently, PTXN treatment blunted GABA-induced upregulation of tight junction proteins in both cell lines. In line with the *in vivo* results, activation of $GABA_AR$ by GABA or MUS downregulated CYP2E1 and iNOS expression in ethanol-treated CCD841 (**Figures 6F**) and T84 (Figures **6G**) cells, effects which were attenuated by PTXN treatment.

3.7 Activation of intestinal $GABA_ARs$ reduces ROS production and enhances tight junction protein expressions by inhibiting CYP2E1

We employed siRNA to further demonstrate a role for CYP2E1 in mediating intestinal barrier function improvement by $GABA_ARs$. Immunofluorescent staining results revealed that ethanol treatment significantly increased ROS production, whereas it failed to induce ROS in cells with *Cyp2e1* knockdown as demonstrated in CCD841 (**Figure 7A**) and T84 (**Figure 7B**) cells. Interestingly, in ethanol-exposed cell models with *Cyp2e1* knockdown, GABA intervention did not further decrease intracellular ROS levels. Consistently, Western blot analysis revealed that in ethanol-exposed CCD841 (**Figures 7C**) and T84 (**Figures 7D**) cells with *Cyp2e1* knockdown, GABA treatment did not induce further reductions in iNOS expression. We also demonstrated that a pharmacological inhibition of CYP2E1 using Clomethiazole (CMZ) yielded results similar to those obtained with si-CYP2E1 (**Supplemental Figure 7A-B**). These findings collectively suggest that activation of GABAARs mitigates ROS production by inhibiting CYP2E1. Finally, in both ethanal-treated CCD841 (**Figures 7E**) and T84 (**Figures 7F**) cells with Cyp2e1 knockdown, the expression of intestinal epithelial cell tight junction proteins remained elevated, and GABA treatment did not alter these protein levels. When combined with results from the in vivo model, these results provide robust support for the conclusion that activation of intestinal GABAARs inhibits ethanol-induced CYP2E1 expression, thereby reducing intestinal ROS

production and enhancing the expression of tight junction proteins in ethanol-exposed colon epithelial cells.

3.8 GABA protection against intestinal barrier dysfunction and liver injury in ALD mice is abolished with an intestinal epithelial cell-specific knockout of *Gabra1*

To further substantiate a role for intestinal epithelial $GABA_A$Rs in regulating intestinal permeability in ALD, we employed an AAV-Villin-cre virus to generate an intestine epithelial cell-specific *Gabra1* knockout mouse (*Gabra1*$^{IEC\text{-}KO}$). Three weeks post tail vein injection of AAV-Villin-cre virus, the tissue-specific colonization and efficacy of the *Gabra1* knockout were verified. These mice were then randomly divided into four groups: *Gabra1*$^{fl/fl}$ + EtOH, *Gabra1*$^{IEC\text{-}KO}$ + EtOH, *Gabra1*$^{fl/fl}$ + EtOH + GABA, and *Gabra1*$^{IEC\text{-}KO}$ + EtOH + GABA, and subjected to the Gao-binge ethanol feeding model protocol (**Figure 8A-C**). Only the *Gabra1*$^{fl/fl}$ + EtOH + GABA group showed no mortality during ethanol feeding, while mortality in the other three groups of mice commenced as early as day 13 (**Supplemental Figure 8A**). There were no significant differences in average food intake among the groups (**Supplemental Figure 8B**).

At the completion of this experiment, *Gabra1*$^{IEC\text{-}KO}$ + EtOH + GABA mice exhibited significantly increased liver index (**Supplemental Figure 8C**) and serum ALT levels (**Figure 8E**) as compared to *Gabra1*$^{fl/fl}$ + EtOH + GABA mice. *Gabra1*$^{IEC\text{-}KO}$ ALD mice exhibited elevated liver indices and serum ALT levels regardless of GABA treatment. Results from H&E (**Figure 8D**) and Oil Red O staining (**Figure 8F**) revealed more extensive fat vacuolation was present in the livers of *Gabra1*$^{IEC\text{-}KO}$ + EtOH + GABA mice compared to *Gabra1*$^{fl/fl}$ + EtOH + GABA mice. Serum TG levels corroborated these findings (**Figure 8G**), indicating that intestinal epithelial $GABA_A$Rs are crucial for the GABA response in ALD mice. In terms of intestinal permeability, *Gabra1*$^{IEC\text{-}KO}$ + EtOH + GABA mice showed a significant increase in liver *lactobacilli* abundance, compared to that in the *Gabra1*$^{fl/fl}$ + EtOH + GABA group (**Figure 8H**). Additionally, GABA administration did not result in an upregulation of tight junction proteins in the intestines of *Gabra1*$^{IEC\text{-}KO}$ ALD mice (**Figures 8I**). Furthermore, in *Gabra1*$^{IEC\text{-}KO}$ ALD mice, no statistically significant reductions in intestinal CYP2E1 protein levels were

obtained in response to GABA administration (**Supplemental Figures 8G-H**). Consistently, the GABA-reduced iNOS and 3-NT levels in intestinal tissue of the *Gabra1*$^{fl/fl}$ + EtOH + GABA group was diminished in the *Gabra1*$^{IEC\text{-}KO}$ + EtOH + GABA group (**Supplemental Figures 8I-K**).

Taken together, these findings demonstrate that the absence of intestinal-specific *Gabra1* prevents GABA from improving liver function damage resulting from by increased intestinal permeability in ALD mice. This is attributed, at least in part, to GABA's inability to downregulate intestinal CYP2E1 and oxidative stress levels in ALD mice through $GABA_AR$s.

4 Discussion

To date, alcohol abstinence remains the most effective preventive and therapeutic measure for ALD [33]. However, despite its fundamental role in ALD management, the efficacy of abstinence is often limited by social factors and the dual physiological and psychological dependence on alcohol in individuals [34]. Currently, traditional pharmacotherapeutic agents for ALD, such as glucocorticoids, are associated with certain adverse effects, while the development and approval of novel medications for ALD progresses at a sluggish pace. In this study, we have identified a novel, protective role of the intestinal GABA-$GABA_AR$ system against ethanol-induced intestinal barrier disruption and liver injury. Specifically, GABA administration improved intestinal barrier function by reversing the ethanol-induced upregulation of intestinal CYP2E1, thereby providing therapeutic benefits against ALD through a gut-liver axis mechanism. Mechanistically, GABA downregulates intestinal epithelial CYP2E1 through its activation of $GABA_AR$s, leading to the restoration of tight junction proteins that are disrupted by intestinal oxidative stress. Pharmacological inhibition or genetic silencing of intestinal epithelial $GABA_AR$s abolishes these effects.

Apart from the acetaldehyde dehydrogenase (ALDH) metabolic pathway, the microsomal alcohol oxidizing system (MEOS) contributes to approximately 10% of alcohol metabolism [35]. Elevated oxidative and nitrosative stress levels associated with this pathway constitute key factors in the tissue and organ damage resulting from

chronic and excessive alcohol consumption [36,37]. CYP2E1, an essential enzyme involved in coenzyme-dependent metabolic pathways, is a critical player in this process [38]. Alcohol, as a potent inducer of CYP2E1, upregulates its expression upon chronic and excessive consumption, leading to the generation of significant quantities of ROS and reactive nitrogen species (RNS), as well as the depletion of endogenous protective substances such as glutathione (GSH) [39,40]. ROS further catalyzes the formation of 4-HNE and MDA via lipid peroxidation, which, upon binding to DNA bases, forms carcinogenic exocyclic etheno-DNA adducts, resulting in endoplasmic reticulum stress, mitochondrial dysfunction, and cellular/tissue damage [41]. In addition to its direct effects on the liver, chronic and excessive alcohol consumption is known to impair intestinal barrier function [42,43]. In this regard, long-term alcohol consumption also induces an upregulation of CYP2E1 in the intestines [44]. The resultant oxidative stress disrupts intestinal barrier function, leading to increased intestinal permeability (i.e. leaky gut) [44]. Therefore, effective strategies to inhibit the induction of intestinal CYP2E1 expression and restoration of intestinal barrier function during chronic alcohol intake hold significant promise for the treatment of ALD.

As the primary inhibitory neurotransmitter in the central nervous system, GABA not only regulates central nervous system functions but also exerts significant roles in peripheral tissues and organs [45]. Previous investigations have demonstrated that GABA can reduce levels of serum glutamate pyruvate transaminase, γ-glutamyl transpeptidase, and MDA in mice, while increasing antioxidant enzyme activities, such as superoxide dismutase and glutathione peroxidase. Additionally, GABA has been reported to alleviate liver injury caused by carbon tetrachloride [46]. Moreover, Deng et al. have reported that GABA can mitigate apoptosis of intestinal epithelial cells induced by enterotoxigenic *Escherichia coli* [47]. These findings underscore a significant role for GABA in regulating gastrointestinal pathophysiology. In the present study, we found that GABA enhanced intestinal barrier function through the downregulation of intestinal CYP2E1 as demonstrated in Gao-binge ALD mice. We have also observed that GABA treatment effectively reduced serum ALT levels and liver MDA levels, diminished hepatic lipid accumulation, and downregulated the

expression of inflammatory mediators. These findings indicate that GABA may modulate intestinal permeability through the enzymatic action of CYP2E1 and exert hepatoprotective effects through the gut-liver axis. In support of this hypothesis, are the findings that culturing liver homogenates from mice within *Lactobacillus* culture medium resulted in significant reductions in the translocation of intestinal microbiota to the liver of ALD mice treated with GABA. Under normal conditions, tight junction protein complexes between intestinal epithelial cells create pore channels that allow only small molecules with diameters less than 0.6 nm (e.g. H_2O and Na^+), to pass through, while larger molecular probes such as FITC-dextran are impermeable [48]. Although a pronounced fluorescent signal in the serum of ALD mice was detected following intragastric FITC-dextran administration, this signal was significantly reduced in GABA-treated ALD mice. Combined with 16S rRNA analysis, our findings provide robust evidence that GABA enhances intestinal barrier function in ALD mice and mitigates intestinal permeability. Additionally, we observed that alcohol consumption significantly inhibits expressions of the intestinal tight junction proteins Occludin, Claudin1 and Claudin4. In contrast, GABA-treated mice exhibit a significant upregulation in the expression of these tight junction proteins, highlighting the capacity for GABA to exert protective effects on intestinal barrier function. Alcohol-induced intestinal permeability can involve a variety of mechanisms, with one such notable mechanism being an alcohol-induced upregulation of intestinal CYP2E1. This upregulation of CYP2E1 can then increase oxidative stress levels and disrupts tight junction proteins [49,50]. In support of this proposal are the findings that inhibitors of CYP2E1 or iNOS can prevent alcohol-induced intestinal permeability, and that CYP2E1 gene-deficient mice demonstrate a significant resistance to this condition [51]. Remarkably, our results revealed that GABA significantly downregulates intestinal CYP2E1 levels and reduces oxidative/nitrosative stress in ALD mice. We therefore propose that the reduction of intestinal CYP2E1 in GABA-treated ALD mice may be a key mechanism underlying the improvements in both intestinal barrier function and liver function observed in these mice.

The $GABA_A$Rs, as the primary target of alcohol's action within the central nervous

system, play a key role in the development of neurologically related symptoms. This receptor is a pentameric chloride ion channel composed of 19 distinct subunits (α1-6, β1-3, γ1-3, δ, ε, θ, π, and ρ1-3) [52-54]. There is considerable evidence indicating that the $GABA_AR$α1 subunit plays a role in modulating sedation, antiepileptic effects, and anterograde amnesia, while the α4 subunit has been implicated in modulating emotional and anxiety-related responses [55]. Functioning as a positive allosteric modulator of $GABA_AR$, alcohol binds to several subunits, including the α subunit, thereby augmenting the transmission of inhibitory neurotransmitters. Such effects are consistent with the reports of sedation, motor coordination impairment and anticonvulsant properties that can be induced by $GABA_AR$ agonists [56]. Additionally, chronic ethanol exposure results in a notable decrease in synaptic $GABA_AR$ α1 subunit, while the α4 subunit are increased [57]. Bearing these in mind, we proposed that GABA's beneficial effects on intestinal-related phenotypes are mediated through $GABA_ARs$. Initially, we assessed the expression of 19 $GABA_AR$ subunits in the colonic tissue of ALD mice and found a significant reduction in *Gabra1* mRNA expression following chronic alcohol consumption, results which were consistent with the findings of Papadeas et. al [58]. This suggests that alcohol's intestinal effects may involve signal transduction mediated by the intestinal GABA signaling system.

As an approach to substantiate this hypothesis, ALD mice were treated with the non-competitive inhibitor of $GABA_AR$, PTXN, to determine whether GABA would remain capable of exerting therapeutic effects. We found that PTXN administration abolished the beneficial effects in GABA-treated ALD mice. Additionally, inhibition of $GABA_AR$ function in ALD mice revealed that GABA did not ameliorate intestinal permeability, which was primarily indicated by reductions in the expressions of tight junction proteins. However, PTXN alone did not worsen intestinal permeability beyond the levels observed in ALD mice, suggesting that endogenous $GABA_ARs$ have a limited protective effect on intestinal permeability in ALD mice. Interestingly, results from a recent study have suggested that while GABA and activated intestinal $GABA_AR$ could reduce the secretion of pro-inflammatory factors such as TNF-α and INF-γ [58], these pro-inflammatory factors might impair the mechanical barrier in DSS-induced acute

637 colitis mouse models. This contrasts with our findings regarding the effects of GABA
638 and intestinal $GABA_AR$s on the intestinal barrier. We attribute this discrepancy to
639 variations in the severity of inflammation and the underlying pathogenic mechanisms
640 across various intestinal diseases. The balance between pro- and anti-inflammatory
641 activities is a dynamic process, where chronic inflammation can lead to conditions such
642 as cancer and fibrosis. However, the effects of inflammation may vary depending on
643 the specific context in which it occurs [59]. In ALD, the intestines exhibit a mild
644 inflammatory response, with infiltrating immune cells capable of producing enough
645 cytokines to remove harmful bacteria and prevent severe tissue damage [60]. In contrast,
646 in acute colitis mouse models, GABA reduces the levels of pro-inflammatory factors,
647 which may hinder the effective elimination of bacteria and contribute to the
648 histopathological damage observed within the colon. Our assessments of colonic
649 CYP2E1 levels and the oxidative stress observed in ALD mice provide strong evidence
650 that activation of $GABA_AR$ could reduce both colonic CYP2E1 levels and oxidative
651 stress, thereby improving intestinal barrier function.

652 To further validate results from our *in vivo* experiments and delineate the cellular
653 target through which GABA exerts its actions, we initially verified the presence of 19
654 $GABA_AR$ subunits in cell lines derived from human colonic epithelia, namely CCD841
655 and T84. In addition to results as obtained with the antagonism of $GABA_AR$ function,
656 direct activation via MUS yielded results congruent with GABA intervention,
657 underscoring a pivotal role for $GABA_AR$s as opposed to that involving alternative
658 receptor subtypes or pathways. Subsequent efforts focused on the inhibiting cellular
659 CYP2E1 through pharmacological and genetic approaches, revealing that alcohol-
660 induced stimulation failed to elevate intracellular ROS. Moreover, co-incubation with
661 GABA did not lead to any further reduction in ROS levels. This underscores the
662 centrality of intestinal epithelial cell CYP2E1 as a critical target for GABA in
663 modulating intestinal barrier functionality.

664 Previous studies have indicated that over 50% of $GABA_AR$s incorporate the α1
665 subunit, which is prominently distributed across a variety of regions within the adult
666 brain [61]. Recent studies have demonstrated significant alterations in intestinal

epithelial $GABA_AR$ α1 expression in models of chemotherapy-induced intestinal injury, implicating its role in injury progression [61]. Our findings of substantial downregulations in *Gabra1* mRNA within the intestines of ALD mice, indicates an involvement of α1 subunits in intestinal changes associated with ALD. This background information prompted us to further explore this issue. To accomplish this goal, we generated an intestinal epithelial cell-specific *Gabra1* knockout mouse using AAV-Villin-cre viral constructs [62]. In this way, it would be possible to determine whether intestinal $GABA_ARs$ are involved in the protective effects of GABA against ethanol-induced intestinal dysfunction and liver injury. Notably, GABA administration failed to ameliorate hepatic function or intestinal barrier integrity in $Gabra1^{IEC\text{-}KO}$ ALD mice, nor did it affect intestinal CYP2E1 or oxidative stress levels. This clearly substantiates a crucial role for the intestinal GABA-$GABA_ARs$ system in the protection against ethanol-induced disruption of intestinal barrier and liver injury.

However, the mechanisms through which epithelial $GABA_ARs$ regulate intestinal CYP2E1 expression remains to be elucidated. GABARAP, a subunit of the $GABA_AR$ complex, is a member of the mammalian Atg8 family and plays a role in autophagosomes and lysosomes formation, transport, and fusion, as well as in the regulation of immune and inflammatory responses, tumor cell growth, metastasis, drug resistance, neurodegenerative diseases, and cardiovascular disease development [63-66]. We initially examined the expression levels of GABARAP family proteins and observed that, compared to the control group, GABARAPL2 expression was significantly increased in the colon of the EtOH group, while these GABARAPL2 levels were restored in the colons of ALD mice treated with GABA. As GABARAP has been shown to regulate the ubiquitination and degradation of certain proteins [66], further research will be required to determine whether $GABA_AR$-induced upregulation of GABARAPL2 disrupts the stability of CYP2E1 through ubiquitination-mediated mechanisms, leading to its subsequent downregulation at the protein level.

In summary, our findings provide strong evidence that activation of the intestinal epithelial GABA-$GABA_ARs$ signaling system plays a crucial protective role against ethanol-induced intestinal barrier dysfunction and liver damage. As summarized in

Figure 9, ethanol increases intestinal CYP2E1 and oxidative stress, leading to the disruption of tight junction proteins, thus enhancing intestinal permeability and exacerbating the progression of ALD. In contrast, GABA treatment targets epithelial $GABA_AR$s, resulting in a downregulation of intestinal CYP2E1 and oxidative stress and subsequently enhancing the tight junction proteins. Such mechanisms assist in maintaining the integrity of intestinal epithelial cells and alleviate ALD. Therefore, our results suggest that GABA treatment offers significant potential as both a dietary intervention and pharmacological agent for the prevention and treatment of ALD and other conditions associated with intestinal barrier dysfunction.

Funding support

The study was supported by grants from the National Natural Science Foundation of China (No. 32371175), and the Key Project of Shandong Province Medical and Health Science and Technology Development Program (No. 202403030318).

Authors' contributions

Lushun Ma, Tianxing Ren, Haojie Zhang, Chuanyong Liu, and Shuanglian Wang conceived the idea and study design, analyzed, interpreted the data, and drafted the manuscript; Chuanyong Liu and Shuanglian Wang obtained the funding support. Jingyi He, Wenshan Jiang, Liying Fang, Zinuo Zhang, Yuanhao Cui, Song Wang, and Daqing Sun helped with administrative, materials, and technical support. Xinyu Ge, Yan Yu, Luoting Guo, Bowen Liu, and Jingyi He were responsible for the revision of manuscripts and figures.

Data availability

Original raw data is available from the corresponding author upon reasonable request.

Conflict of interest

The authors declare that there is no conflict of interest in this study.

References

[1] X. Wu, X. Fan, T. Miyata, A. Kim, R.C. Cajigas-Du, S. Ray, E. Huang, M. Taiwo, R. Arya, J. Wu, L.E. Nagy, Recent advances in understanding of pathogenesis of alcohol-associated liver disease, Annu. Rev. Pathol.-Mech Dis. 18 (2023) 411-438.

[2] H.K. Seitz, R. Bataller, H. Cortez-Pinto, B. Gao, A. Gual, C. Lackner, P. Mathurin, S. Mueller, G. Szabo, H. Tsukamoto, Alcoholic liver disease, Nat. Rev. Dis. Primers 4 (1) (2018) 16.

[3] H. Devarbhavi, S.K. Asrani, J.P. Arab, Y.A. Nartey, E. Pose, P.S. Kamath, Global burden of liver disease: 2023 update, J. Hepatol. 79 (2) (2023) 516-537.

[4] D.Q. Huang, P. Mathurin, H. Cortez-Pinto, R. Loomba, Global epidemiology of alcohol-associated cirrhosis and hcc: trends, projections and risk factors, Nat. Rev. Gastroenterol. Hepatol. 20 (1) (2023) 37-49.

[5] L.A. Diaz, J.P. Arab, A. Louvet, R. Bataller, M. Arrese, The intersection between alcohol-related liver disease and nonalcoholic fatty liver disease, Nat. Rev. Gastroenterol. Hepatol. 20 (12) (2023) 764-783.

[6] G. Szabo, Gut-liver axis in alcoholic liver disease, Gastroenterology 148 (1) (2015) 30-36.

[7] Z. Hou, Q. Ding, Y. Li, Z. Zhao, F. Yan, Y. Li, X. Wang, J. Xu, W. Chen, G. Wu, X. Ruan, L. Zhao, Intestinal epithelial beta klotho is a critical protective factor in alcohol-induced intestinal barrier dysfunction and liver injury, Ebiomedicine 82 (2022) 104181.

[8] P. Chen, P. Starkel, J.R. Turner, S.B. Ho, B. Schnabl, Dysbiosis-induced intestinal inflammation activates tumor necrosis factor receptor i and mediates alcoholic liver disease in mice, Hepatology 61 (3) (2015) 883-894.

[9] R. Rao, Endotoxemia and gut barrier dysfunction in alcoholic liver disease, Hepatology 50 (2) (2009) 638-644.

[10] Y. Duan, C. Llorente, S. Lang, K. Brandl, H. Chu, L. Jiang, R.C. White, T.H. Clarke, K. Nguyen, M. Torralba, Y. Shao, J. Liu, A. Hernandez-Morales, L. Lessor, I.R. Rahman, Y. Miyamoto, M. Ly, B. Gao, W. Sun, R. Kiesel, F. Hutmacher, S. Lee, M. Ventura-Cots, F. Bosques-Padilla, E.C. Verna, J.G. Abraldes, R.J. Brown, V. Vargas, J. Altamirano, J. Caballeria, D.L. Shawcross, S.B. Ho, A. Louvet, M.R. Lucey, P. Mathurin, G. Garcia-Tsao, R. Bataller, X.M. Tu, L. Eckmann, W.A. van der Donk, R. Young, T.D. Lawley, P. Starkel, D. Pride, D.E. Fouts, B. Schnabl, Bacteriophage targeting of gut bacterium attenuates alcoholic liver disease, Nature 575 (7783) (2019) 505-511.

[11] L.X. Yu, R.F. Schwabe, The gut microbiome and liver cancer: mechanisms and clinical translation, Nat. Rev. Gastroenterol. Hepatol. 14 (9) (2017) 527-539.

[12] Y.E. Cho, B.J. Song, Pomegranate prevents binge alcohol-induced gut leakiness and hepatic inflammation by suppressing oxidative and nitrative stress, Redox Biol. 18 (2018) 266-278.

[13] D. Zogona, A.W. Zongo, A.E. Elkhedir, M. Salah, M. Tao, R. Li, T. Wu, X. Xu, Red raspberry supplementation mitigates alcohol-induced liver injury associated with gut microbiota alteration and intestinal barrier dysfunction in mice, Food Funct. 14 (2) (2023) 1209-1226.

[14] Q. Xu, R. Zhang, Y. Mu, Y. Song, N. Hao, Y. Wei, Q. Wang, C.R. Mackay, Propionate ameliorates alcohol-induced liver injury in mice via the gut-liver axis: focus on the improvement of intestinal permeability, J. Agric. Food Chem. 70 (20) (2022) 6084-6096.

[15] L. Milosevic, R. Gramer, T.H. Kim, M. Algarni, A. Fasano, S.K. Kalia, M. Hodaie, A.M. Lozano, M.R. Popovic, W.D. Hutchison, Modulation of inhibitory plasticity in basal ganglia output nuclei of patients with parkinson's disease, Neurobiol. Dis.

784 124 (2019) 46-56.
785 [16] S.B. Sarasa, R. Mahendran, G. Muthusamy, B. Thankappan, D. Selta, J.
786 Angayarkanni, A brief review on the non-protein amino acid, gamma-amino
787 butyric acid (gaba): its production and role in microbes, Curr. Microbiol. 77 (4)
788 (2020) 534-544.
789 [17] S. Zhu, C.M. Noviello, J. Teng, R.J. Walsh, J.J. Kim, R.E. Hibbs, Structure of a
790 human synaptic gaba(a) receptor, Nature 559 (7712) (2018) 67-72.
791 [18] Y. Li, Y.Y. Xiang, W.Y. Lu, C. Liu, J. Li, A novel role of intestine epithelial
792 gabaergic signaling in regulating intestinal fluid secretion, Am. J. Physiol.-
793 Gastroint. Liver Physiol. 303 (4) (2012) G453-G460.
794 [19] C. Zhang, Y. Zhou, J. Zheng, N. Ning, H. Liu, W. Jiang, X. Yu, K. Mu, Y. Li,
795 W. Guo, H. Hu, J. Li, D. Chen, Inhibition of gabaa receptors in intestinal stem
796 cells prevents chemoradiotherapy-induced intestinal toxicity, J. Exp. Med. 219 (12)
797 (2022).
798 [20] M.M. Silveri, Gabaergic contributions to alcohol responsivity during adolescence:
799 insights from preclinical and clinical studies, Pharmacol. Ther. 143 (2) (2014) 197-
800 216.
801 [21] J.R. Trudell, R.O. Messing, J. Mayfield, R.A. Harris, Alcohol dependence:
802 molecular and behavioral evidence, Trends Pharmacol. Sci. 35 (7) (2014) 317-323.
803 [22] T. Ramirez, Y.M. Li, S. Yin, M.J. Xu, D. Feng, Z. Zhou, M. Zang, P.
804 Mukhopadhyay, Z.V. Varga, P. Pacher, B. Gao, H. Wang, Aging aggravates
805 alcoholic liver injury and fibrosis in mice by downregulating sirtuin 1 expression,
806 J. Hepatol. 66 (3) (2017) 601-609.
807 [23] A. Bertola, S. Mathews, S.H. Ki, H. Wang, B. Gao, Mouse model of chronic and
808 binge ethanol feeding (the niaaa model), Nat. Protoc. 8 (3) (2013) 627-637.
809 [24] Raya Tonetti F, Eguileor A, Mrdjen M, Pathak V, Travers J, Nagy LE, Llorente C.
810 Gut-liver axis: Recent concepts in pathophysiology in alcohol-associated liver
811 disease. Hepatology. 2024 Dec 1;80(6):1342-1371.
812 [25] J. Ewaschuk, R. Endersby, D. Thiel, H. Diaz, J. Backer, M. Ma, T. Churchill, K.
813 Madsen, Probiotic bacteria prevent hepatic damage and maintain colonic barrier

function in a mouse model of sepsis, Hepatology 46 (3) (2007) 841-850.
[26] M.A. Abdelmegeed, A. Banerjee, S. Jang, S.H. Yoo, J.W. Yun, F.J. Gonzalez, A. Keshavarzian, B.J. Song, Cyp2e1 potentiates binge alcohol-induced gut leakiness, steatohepatitis, and apoptosis, Free Radic. Biol. Med. 65 (2013) 1238-1245.
[27] D. Zhang, Z. Liu, F. Bai, Roles of gut microbiota in alcoholic liver disease, Int. J. Gen. Med. 16 (2023) 3735-3746.
[28] S. Prabhulkar, C.Z. Li, Assessment of oxidative dna damage and repair at single cellular level via real-time monitoring of 8-ohdg biomarker, Biosens. Bioelectron. 26 (4) (2010) 1743-1749.
[29] E. Gatta, D. Camussi, J. Auta, A. Guidotti, S.C. Pandey, Neurosteroids (allopregnanolone) and alcohol use disorder: from mechanisms to potential pharmacotherapy, Pharmacol. Ther. 240 (2022) 108299.
[30]J. Liang, R.W. Olsen, Alcohol use disorders and current pharmacological therapies: the role of gaba(a) receptors, Acta Pharmacol. Sin. 35 (8) (2014) 981-993.
[31] D.G. McEwan, D. Popovic, A. Gubas, S. Terawaki, H. Suzuki, D. Stadel, F.P. Coxon, D.S.D. Miranda, S. Bhogaraju, K. Maddi, A. Kirchof, E. Gatti, M.H. Helfrich, S. Wakatsuki, C. Behrends, P. Pierre, I. Dikic, Plekhm1 regulates autophagosome-lysosome fusion through hops complex and lc3/gabarap proteins, Mol. Cell 57 (1) (2015) 39-54.
[32] H.M. Genau, J. Huber, F. Baschieri, M. Akutsu, V. Dotsch, H. Farhan, V. Rogov, C. Behrends, Cul3-kbtbd6/kbtbd7 ubiquitin ligase cooperates with gabarap proteins to spatially restrict tiam1-rac1 signaling, Mol. Cell 57 (6) (2015) 995-1010.
[33] B.S. Hofer, B. Simbrunner, L. Hartl, M. Jachs, D. Bauer, L. Balcar, R. Paternostro, P. Schwabl, G. Semmler, B. Scheiner, A.F. Staettermayer, M. Trauner, M. Mandorfer, T. Reiberger, Alcohol abstinence improves prognosis across all stages of portal hypertension in alcohol-related cirrhosis, Clin. Gastroenterol. Hepatol. 21 (9) (2023) 2308-2317.
[34] R. Parker, S.J. Kim, B. Gao, Alcohol, adipose tissue and liver disease: mechanistic links and clinical considerations, Nat. Rev. Gastroenterol. Hepatol. 15 (1) (2018)

844 50-59.
845 [35] S. Zakhari, Overview: how is alcohol metabolized by the body? Alcohol Res.-Curr.
846 Rev. 29 (4) (2006) 245-254.
847 [36] A. Allameh, R. Niayesh-Mehr, A. Aliarab, G. Sebastiani, K. Pantopoulos,
848 Oxidative stress in liver pathophysiology and disease, Antioxidants 12 (9) (2023).
849 [37] H. Tilg, A.R. Moschen, N.C. Kaneider, Pathways of liver injury in alcoholic liver
850 disease, J. Hepatol. 55 (5) (2011) 1159-1161.
851 [38] Y.E. Cho, E. Mezey, J.P. Hardwick, N.J. Salem, D.L. Clemens, B.J. Song,
852 Increased ethanol-inducible cytochrome p450-2e1 and cytochrome p450 isoforms
853 in exosomes of alcohol-exposed rodents and patients with alcoholism through
854 oxidative and endoplasmic reticulum stress, Hepatol. Commun. 1 (7) (2017) 675-
855 690.
856 [39] A.A. Caro, A.I. Cederbaum, Oxidative stress, toxicology, and pharmacology of
857 cyp2e1, Annu. Rev. Pharmacol. Toxicol. 44 (2004) 27-42.
858 [40] Y. Lu, A.I. Cederbaum, Cyp2e1 and oxidative liver injury by alcohol, Free Radic.
859 Biol. Med. 44 (5) (2008) 723-738.
860 [41] K. Linhart, H. Bartsch, H.K. Seitz, The role of reactive oxygen species (ros) and
861 cytochrome p-450 2e1 in the generation of carcinogenic etheno-dna adducts,
862 Redox Biol. 3 (2014) 56-62.
863 [42] J. Martel, S.H. Chang, Y.F. Ko, T.L. Hwang, J.D. Young, D.M. Ojcius, Gut barrier
864 disruption and chronic disease, Trends Endocrinol. Metab. 33 (4) (2022) 247-265.
865 [43] X. Wu, X. Fan, T. Miyata, A. Kim, R.C. Cajigas-Du, S. Ray, E. Huang, M. Taiwo,
866 R. Arya, J. Wu, L.E. Nagy, Recent advances in understanding of pathogenesis of
867 alcohol-associated liver disease, Annu. Rev. Pathol.-Mech Dis. 18 (2023) 411-438.
868 [44] M.A. Abdelmegeed, A. Banerjee, S. Jang, S.H. Yoo, J.W. Yun, F.J. Gonzalez, A.
869 Keshavarzian, B.J. Song, Cyp2e1 potentiates binge alcohol-induced gut leakiness,
870 steatohepatitis, and apoptosis, Free Radic. Biol. Med. 65 (2013) 1238-1245.
871 [45] S.S. Roberts, M.C. Mendonca-Torres, K. Jensen, G.L. Francis, V. Vasko, Gaba
872 receptor expression in benign and malignant thyroid tumors, Pathol. Oncol. Res.
873 15 (4) (2009) 645-650.

[46] B.J. Lee, M. Senevirathne, J.S. Kim, Y.M. Kim, M.S. Lee, M.H. Jeong, Y.M. Kang, J.I. Kim, B.H. Nam, C.B. Ahn, J.Y. Je, Protective effect of fermented sea tangle against ethanol and carbon tetrachloride-induced hepatic damage in sprague-dawley rats, Food Chem. Toxicol. 48 (4) (2010) 1123-1128.

[47] Y. Xia, S. Chen, Y. Zhao, S. Chen, R. Huang, G. Zhu, Y. Yin, W. Ren, J. Deng, Gaba attenuates etec-induced intestinal epithelial cell apoptosis involving gaba(a)r signaling and the ampk-autophagy pathway, Food Funct. 10 (11) (2019) 7509-7522.

[48] A. Horowitz, S.D. Chanez-Paredes, X. Haest, J.R. Turner, Paracellular permeability and tight junction regulation in gut health and disease, Nat. Rev. Gastroenterol. Hepatol. 20 (7) (2023) 417-432.

[49] C.B. Forsyth, R.M. Voigt, A. Keshavarzian, Intestinal cyp2e1: a mediator of alcohol-induced gut leakiness, Redox Biol. 3 (2014) 40-46.

[50] C.B. Forsyth, R.M. Voigt, M. Shaikh, Y. Tang, A.I. Cederbaum, F.W. Turek, A. Keshavarzian, Role for intestinal cyp2e1 in alcohol-induced circadian gene-mediated intestinal hyperpermeability, Am. J. Physiol.-Gastroint. Liver Physiol. 305 (2) (2013) G185-G195.

[51] B.T. Davis, R.M. Voigt, M. Shaikh, C.B. Forsyth, A. Keshavarzian, Creb protein mediates alcohol-induced circadian disruption and intestinal permeability, Alcoholism (Ny) 41 (12) (2017) 2007-2014.

[52] S.N. Boehm, I. Ponomarev, A.W. Jennings, P.J. Whiting, T.W. Rosahl, E.M. Garrett, Y.A. Blednov, R.A. Harris, Gamma-aminobutyric acid a receptor subunit mutant mice: new perspectives on alcohol actions, Biochem. Pharmacol. 68 (8) (2004) 1581-1602.

[53] G.F. Koob, A role for gaba mechanisms in the motivational effects of alcohol, Biochem. Pharmacol. 68 (8) (2004) 1515-1525.

[54] M.M. Silveri, Gabaergic contributions to alcohol responsivity during adolescence: insights from preclinical and clinical studies, Pharmacol. Ther. 143 (2) (2014) 197-216.

[55] A. Sente, R. Desai, K. Naydenova, T. Malinauskas, Y. Jounaidi, J. Miehling, X.

Zhou, S. Masiulis, S.W. Hardwick, D.Y. Chirgadze, K.W. Miller, A.R. Aricescu, Differential assembly diversifies gaba(a) receptor structures and signalling, Nature 604 (7904) (2022) 190-194.

[56] U. Rudolph, F. Knoflach, Beyond classical benzodiazepines: novel therapeutic potential of gabaa receptor subtypes, Nat. Rev. Drug Discov. 10 (9) (2011) 685-697.

[54] S.L. Carlson, J.P. Bohnsack, A.L. Morrow, Ethanol regulation of synaptic gabaa alpha4 receptors is prevented by protein kinase a activation, J. Pharmacol. Exp. Ther. 357 (1) (2016) 10-16.

[58] S. Papadeas, A.C. Grobin, A.L. Morrow, Chronic ethanol consumption differentially alters gaba(a) receptor alpha1 and alpha4 subunit peptide expression and gaba(a) receptor-mediated 36 cl(-) uptake in mesocorticolimbic regions of rat brain, Alcoholism (Ny) 25 (9) (2001) 1270-1275.

[59] S.J. McElroy, L.S. Prince, J.H. Weitkamp, J. Reese, J.C. Slaughter, D.B. Polk, Tumor necrosis factor receptor 1-dependent depletion of mucus in immature small intestine: a potential role in neonatal necrotizing enterocolitis, Am. J. Physiol.-Gastroint. Liver Physiol. 301 (4) (2011) G656-G666.

[60] M. Meroni, M. Longo, P. Dongiovanni, Alcohol or gut microbiota: who is the guilty? Int. J. Mol. Sci. 20 (18) (2019).

[61] S. Kumar, P. Porcu, D.F. Werner, D.B. Matthews, J.L. Diaz-Granados, R.S. Helfand, A.L. Morrow, The role of gaba(a) receptors in the acute and chronic effects of ethanol: a decade of progress, Psychopharmacology 205 (4) (2009) 529-564.

[62] Z. Hou, Q. Ding, Y. Li, Z. Zhao, F. Yan, Y. Li, X. Wang, J. Xu, W. Chen, G. Wu, X. Ruan, L. Zhao, Intestinal epithelial beta klotho is a critical protective factor in alcohol-induced intestinal barrier dysfunction and liver injury, Ebiomedicine 82 (2022) 104181.

[63] C. Vianello, M. Salluzzo, D. Anni, D. Boriero, M. Buffelli, L. Carboni, Increased expression of autophagy-related genes in alzheimer's disease-type 2 diabetes mellitus comorbidity models in cells, Int. J. Environ. Res. Public Health 20 (5)

(2023).
[64] J. Chen, H. Zhao, M. Liu, L. Chen, A new perspective on the autophagic and non-autophagic functions of the gabarap protein family: a potential therapeutic target for human diseases, Mol. Cell. Biochem. 479 (6) (2024) 1415-1441.
[65] E. Hervouet, A. Claude-Taupin, T. Gauthier, V. Perez, A. Fraichard, P. Adami, G. Despouy, F. Monnien, M.P. Algros, M. Jouvenot, R. Delage-Mourroux, M. Boyer-Guittaut, The autophagy gabarapl1 gene is epigenetically regulated in breast cancer models, Bmc Cancer 15 (2015) 729.
[66] E. Cagetti, J. Liang, I. Spigelman, R.W. Olsen, Withdrawal from chronic intermittent ethanol treatment changes subunit composition, reduces synaptic function, and decreases behavioral responses to positive allosteric modulators of gabaa receptors, Mol. Pharmacol. 63 (1) (2003) 53-64.

Figure 1. GABA ameliorates liver function damage in Gao-binge ALD mice.
(A) Chronic-plus-single-binge alcohol feeding protocol for establishing the Gao-binge ALD mouse model. GABA (daily i.p. 200 mg/kg) was administered according to mice in the indicated groups. (B) Food intake and (C) body weight of mice within each group during generation of the model. (D) Comparative analysis of liver index and (E) serum ALT levels within the different groups (n=5-6/group). (F) The level of LPS in portal vein serum. (n=5-6/group).(G and H) Histological examination of mouse liver tissues via H&E (G) and Oil Red O (H) staining revealed increased lipid vacuoles in the EtOH group. (I and J) Determination of hepatic TG (I) and liver tissue MDA (J) levels (n=6/group). (K) RT-PCR analysis of inflammatory factors IL-1β, TNF-α, and IL-6 expression in mice liver (n=6/group). Significance levels denoted as $*P < 0.05$, $**P < 0.01$, $***P < 0.001$, $****P < 0.0001$, ns, not statistically significant.

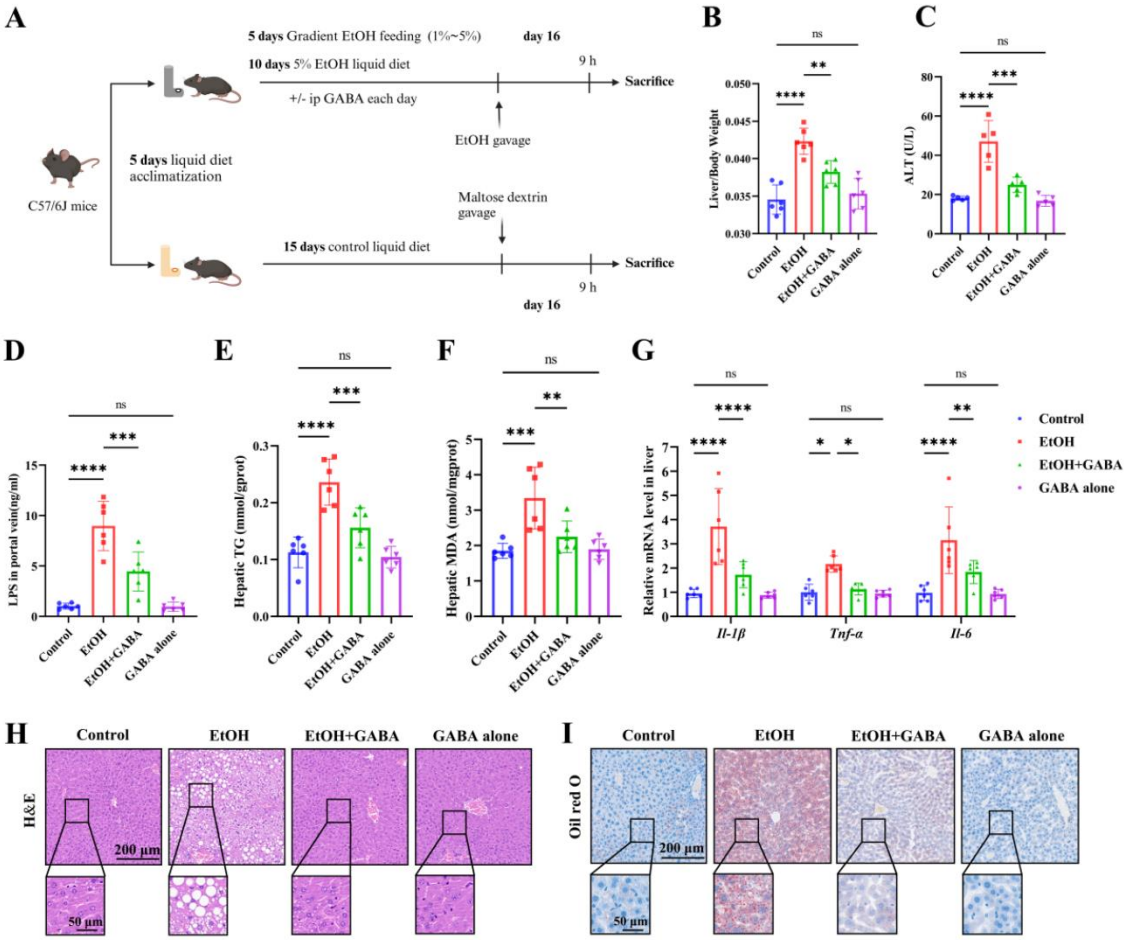

Figure 1. GABA ameliorates liver function damage in Gao-binge ALD mice.

(A) Chronic-plus-single-binge alcohol feeding protocol for establishing the Gao-binge ALD mouse model. GABA (daily i.p. 200 mg/kg) was administered according to mice in the indicated groups. (B) Comparative analysis of liver index and (C) serum ALT levels within the different groups (n=5-6/group). (D) The level of LPS in portal vein serum. (n=5-6/group). (E and F) Determination of hepatic TG (E) and liver tissue MDA (F) levels (n=6/group). (G) RT-PCR analysis of inflammatory factors IL-1β, TNF-α, and IL-6 expression in mice liver (n=6/group). (H and I) Histological examination of mouse liver tissues via H&E (H) and Oil Red O (I) staining revealed increased lipid vacuoles in the EtOH group.Significance levels denoted as $*P < 0.05$, $**P < 0.01$, $***P < 0.001$, $****P < 0.0001$, ns, not statistically significant.

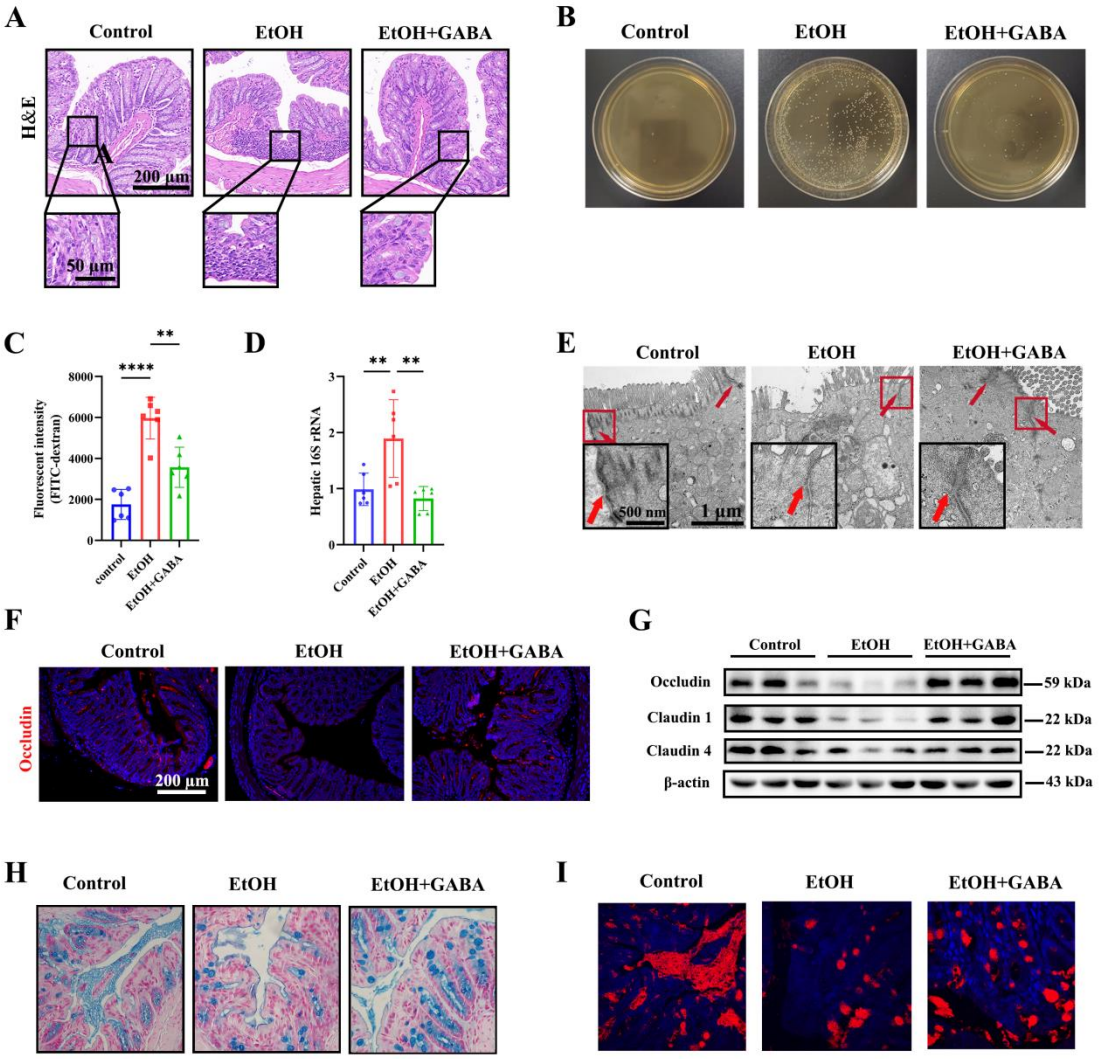

Figure 2. GABA ameliorates intestinal barrier function damage in Gao-binge ALD mice. (A) H&E staining of colon tissues within the EtOH group revealed an increased infiltration of inflammatory cells in the submucosa. (B) Lactobacillus cultures were used to detect colony formation in liver homogenates. (C) Intestinal permeability as assessed with the fluorescein isothiocyanate FITC–dextran test (n=6/group). (D) RT-PCR analysis was performed to investigate the expression profile of 16S rRNA in mouse liver tissues (n=6/group). (E) Transmission electron microscopy was utilized to observe tight junction proteins in colon epithelia of mice, with red arrows and triangles indicating tight junction proteins and black boxes representing the magnified view of the red box. (F) The representative immunofluorescent staining images of tight junction

protein Occludin in mouse colon sections (n=6/group). (G) Western blot analysis of colonic tight junction protein expressions in mice. (H) Alcian blue staining for detection of colonic mucus secretions (blue) in mice. (I) Immunofluorescent staining of MUC2 in a cross-sectional image of the mouse colon (red). Significance levels denoted as *P < 0.05, **P < 0.01, ***P < 0.001, ****P < 0.0001.

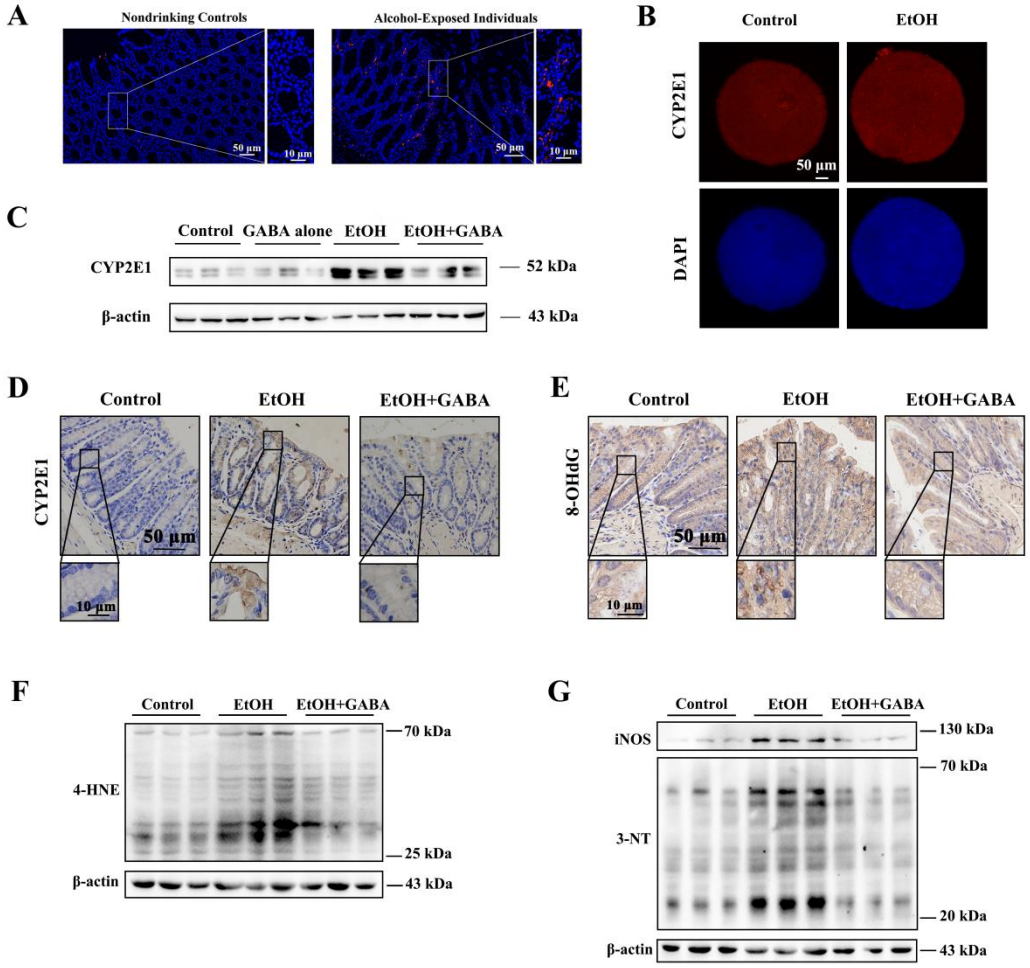

Figure 3. GABA downregulates intestinal CYP2E1 and oxidative stress in Gao-binge ALD mice.

(A) Colonic CYP2E1 expression in nondrinking controls and alcohol-exposed individuals. (B) CYP2E1 immunofluorescence in mouse colon organoids following ethanol stimulation. (C) Western blot analysis of intestinal CYP2E1 expression. (D) Representative immunohistochemical staining images of CYP2E1 in colonic sections of mice (n=10/group). (E) Representative immunohistochemical staining images of 8-OHdG in colonic sections (n=10/group). (F and G) Western blot analysis of intestinal expression of 4-HNE, iNOS and 3-NT. Significance levels denoted as *P < 0.05, **P < 0.01.

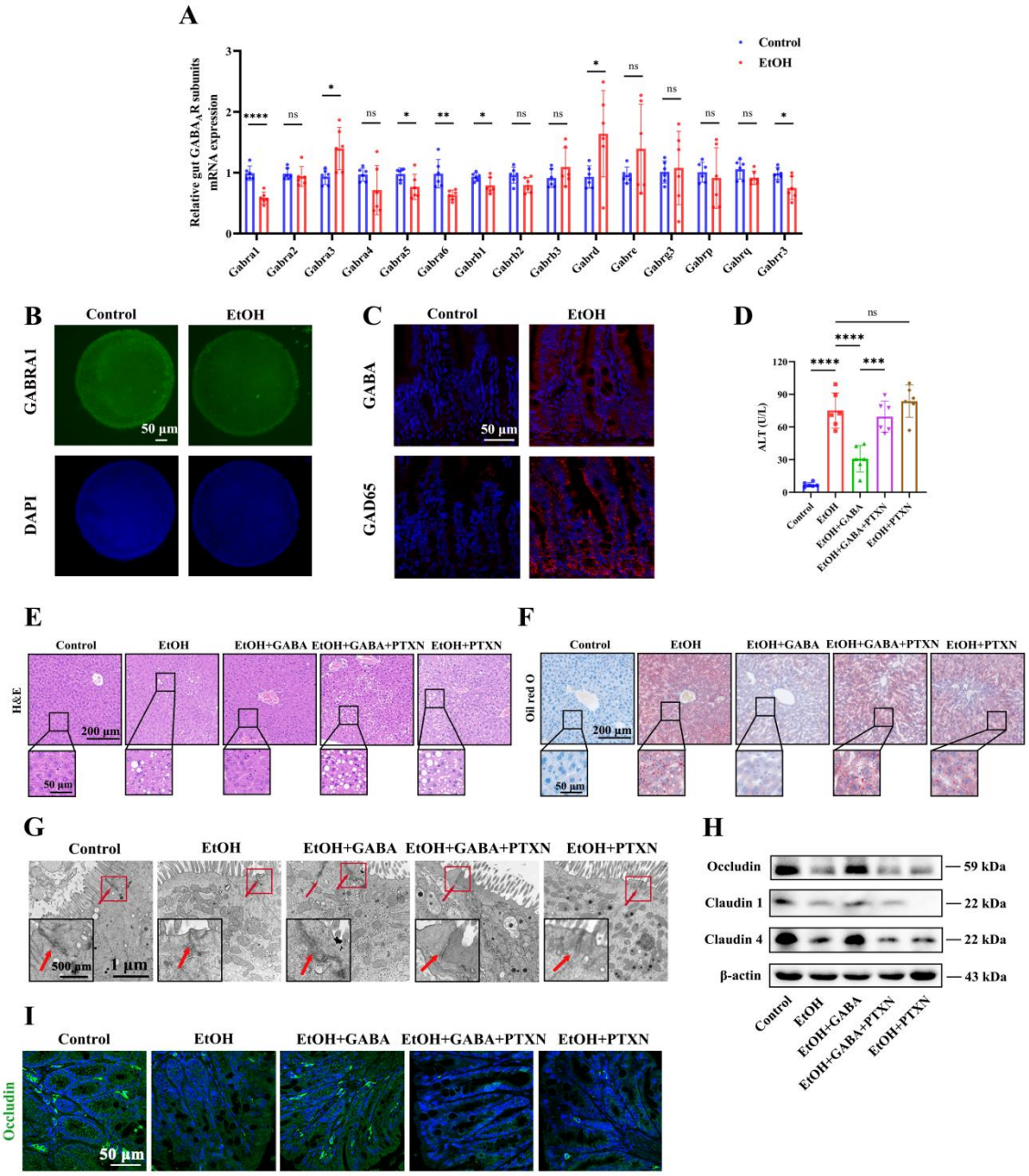

Figure 4. Effect of intestinal GABAARs on Gao-binge ALD mouse model phenotype. (A) RT-PCR analysis of GABAAR subunit gene expressions in colons of control and ALD mice. During ALD modeling process, mice were treated with GABA (daily i.p. 200 mg/kg) or the GABAAR antagonist, picrotoxin (PTXN, bi-daily i.p. 2mg / kg) (n=6/group). (B) GABRA1 immunofluorescence in mouse colon organoids following ethanol stimulation. (C) Representative immunofluorescent staining images of GABA and GAD65 in mouse colon sections. (D) Comparative analysis of serum ALT levels within the different groups (n=6/group). (E and F) Histological examination of mouse

liver tissues via H&E (E) and Oil Red O (F) staining. (G) Transmission electron microscopy was utilized to observe tight junction proteins in colon epithelium, with red arrows and triangles indicating tight junction proteins and black boxes representing the magnified view of the red box. (H) Western blot analysis for determining the expression of colonic tight junction proteins in mice. (I) Representative immunofluorescent staining images of tight junction protein Occludin in mouse colon sections (n=10/group). Significance levels denoted as *P < 0.05, **P < 0.01, ***P < 0.001, ****P < 0.0001, ns, not statistically significant.

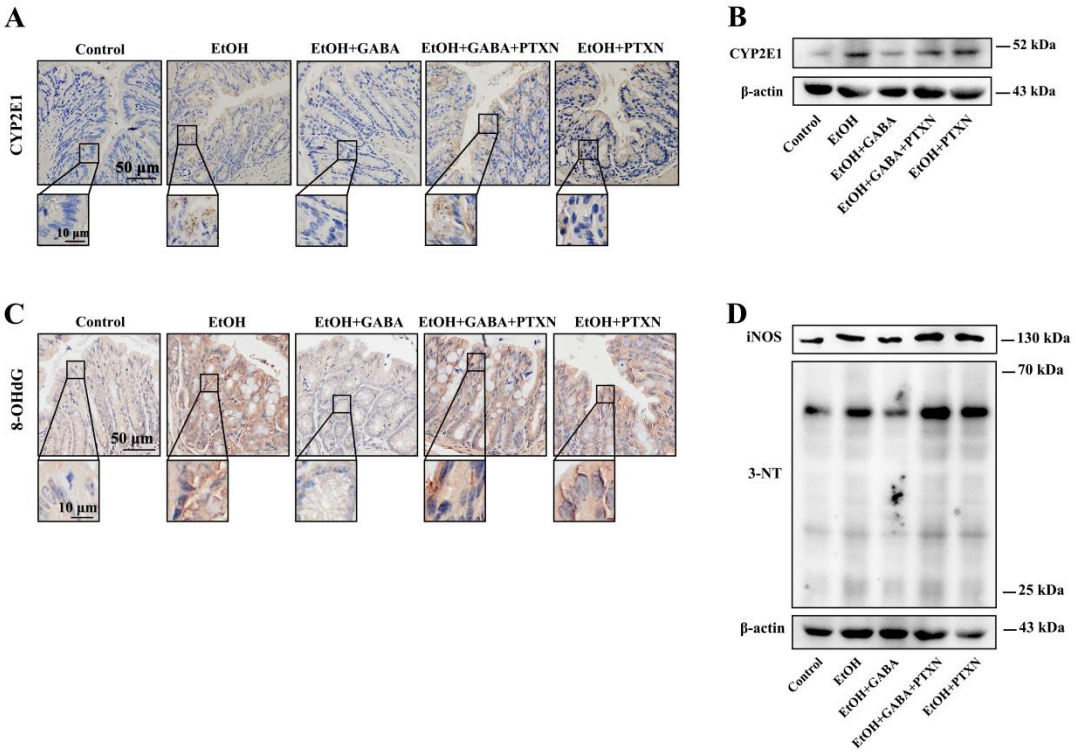

Figure 5. GABA mediates the downregulation of intestinal CYP2E1 and oxidative stress through GABAARs.

(A) Representative immunohistochemical staining images of CYP2E1 in colonic sections of mice. (B) Western blot analysis for determining intestinal CYP2E1 expression. (C) Representative immunohistochemical staining images of 8-OHdG in colonic sections of mice. (D) Western blot analysis of oxidative stress-related proteins in the colons of mice. Significance levels denoted as *P < 0.05, **P < 0.01, ***P < 0.001, ns, not statistically significant.

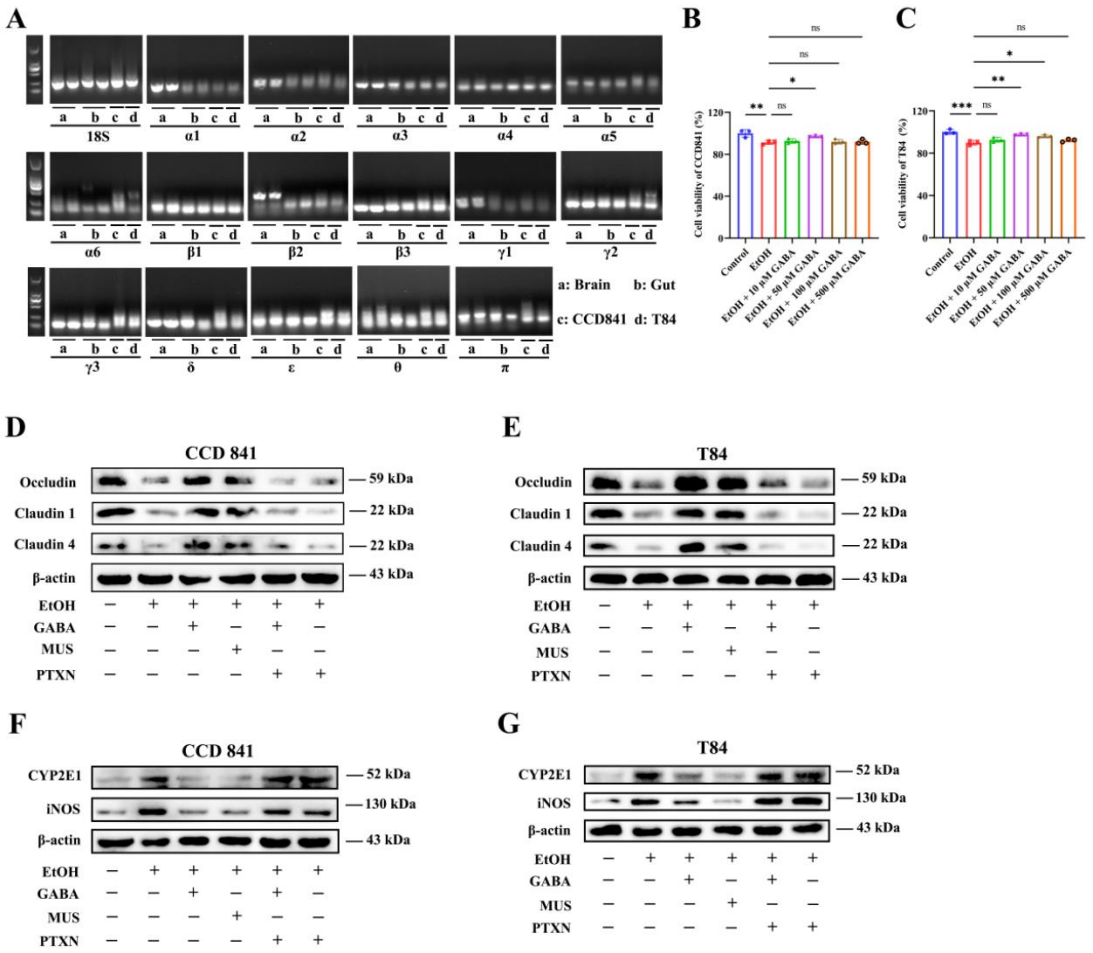

Figure 6. GABA upregulates tight junction protein expressions by downregulating CYP2E1 expression via $GABA_AR$ in the intestinal epithelial cells.

(A) PCR was used to detect the presence of 19 $GABA_AR$ subunits in CCD841 and T84 cells: a) Mouse cortical tissue was used as a positive control, b) Mouse colon tissue, c) CCD841 cells and d) T84 cells. (B and C) CCD841 (B) and T84 (C) cells were stimulated with 80 mM ethanol for 48 h, while simultaneously incubated with GABA at concentrations ranging from 10 to 500 μM (n=3/group). (D) Western Blot analyses of expression changes of tight junction proteins in ethanol-challenged CCD841 cells treated with GABA (50 μM), the $GABA_AR$ agonist, MUS (100 μM), or the $GABA_AR$ antagonist, PTXN (100 μM) (n=3/group). (E) Western Blot analyses of expression changes of tight junction proteins in ethanol-challenged T84 cells treated with GABA

(50 μM), the $GABA_AR$ agonist, MUS (100 μM), or the $GABA_AR$ antagonist, PTXN (100 μM). (F) Western Blot analyses of CYP2E1 and iNOS expression changes in ethanol-challenged CCD841 cells. (G) Western Blot analyses of CYP2E1 and iNOS expression changes in ethanol-challenged T84 cells. Significance levels denoted as $*P < 0.05$, $**P < 0.01$, $***P < 0.001$, $****P < 0.0001$, ns, not statistically significant. Each experiment was performed in triplicate.

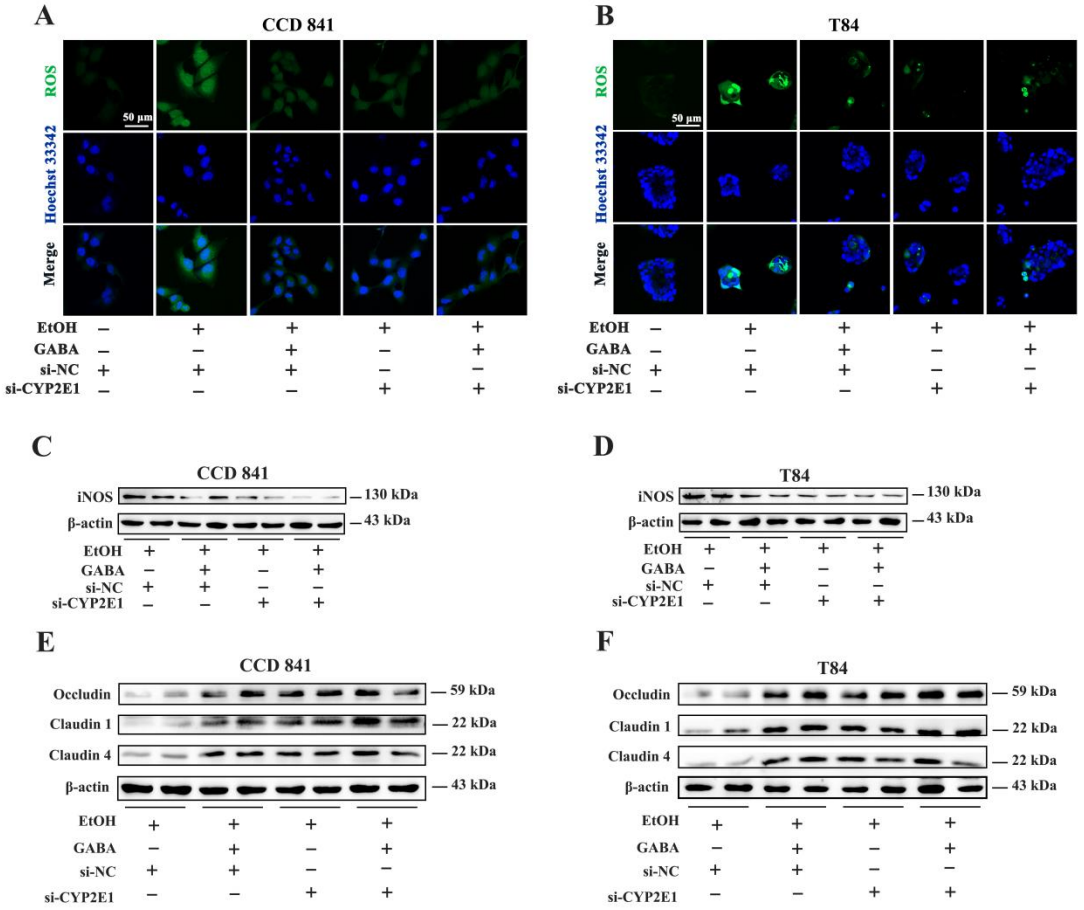

Figure 7. GABA-mediated downregulation of CYP2E1 within ethanol-challenged intestinal epithelial cells mitigates oxidative stress.

(A and B) After transfection with si-CYP2E1 or the siRNA negative control, fluorescent detection was used to determine ROS levels in ethanol-challenged CCD841 (A) and T84 (B) cells (n=6/group). (C) Western Blot analysis of iNOS expression levels in ethanol-challenged CCD841 cells. (D) Western Blot analysis of iNOS expression changes of in ethanol-challenged T84 cells. (E) After transfection of CCD841 cells with si-CYP2E1 or the siRNA negative control, western blot analyses were conducted to

assess changes in the expression of tight junction proteins in ethanol-challenged cells treated with GABA (50 μM). (F) After transfection of T84 cells with si-CYP2E1 or the siRNA negative control, Western blot analyses were conducted to assess changes in the expression of tight junction proteins in ethanol-challenged cells treated with GABA (50 μM). Significance levels denoted as *P < 0.05, **P < 0.01, ***P < 0.001, ****P < 0.0001, ns, not statistically significant. Each experiment was performed at least in triplicate.

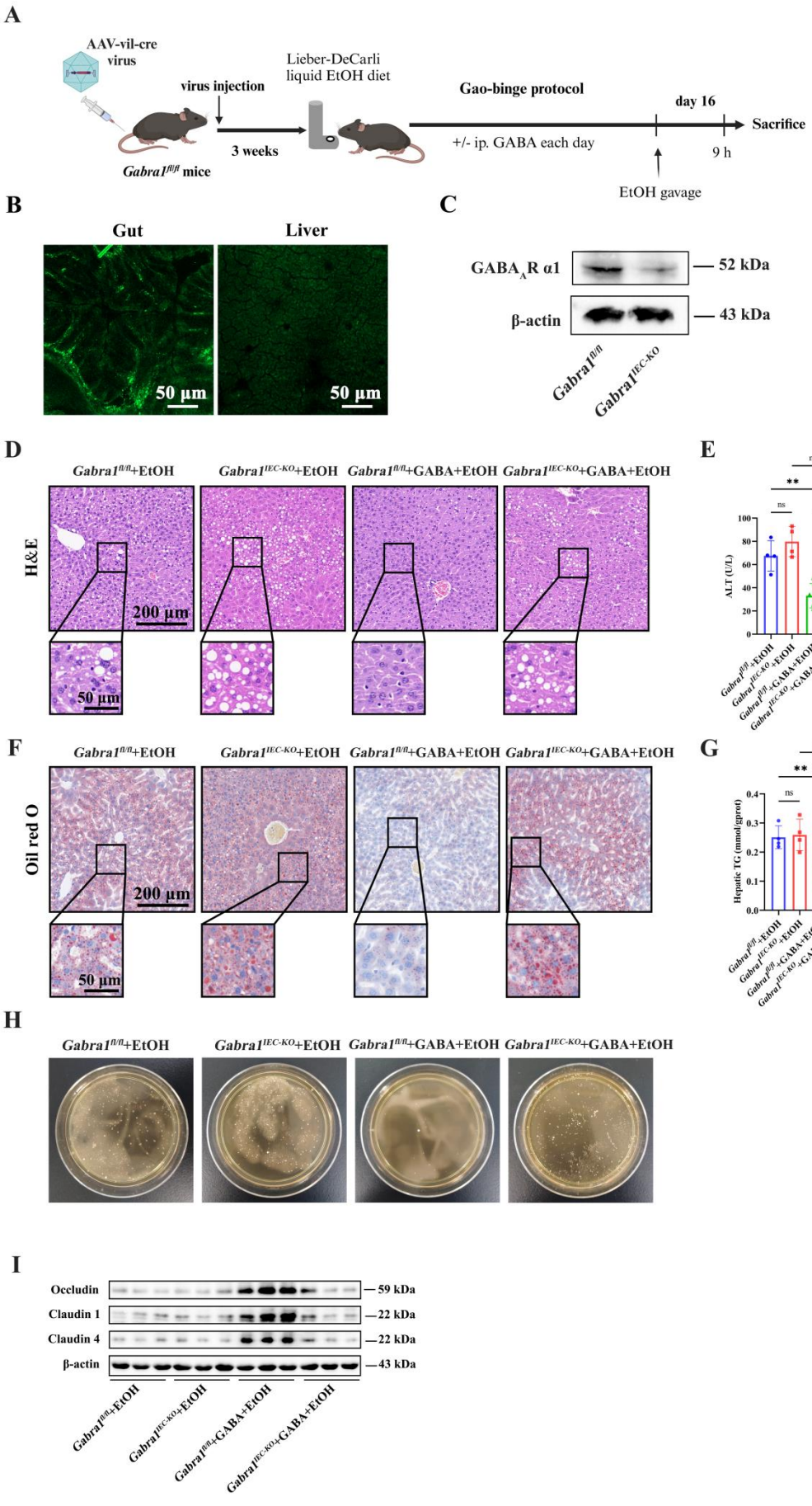
A
AAV-vil-cre virus
virus injection
3 weeks
Gabra1fl/fl mice
Lieber-DeCarli liquid EtOH diet
Gao-binge protocol
day 16
Sacrifice
+/- ip. GABA each day
9 h
EtOH gavage
B
Gut
Liver
50 μm
50 μm
C
GABAAR α1
52 kDa
β-actin
43 kDa
Gabra1fl/fl
Gabra1IEC-KO
D
Gabra1fl/fl+EtOH
Gabra1IEC-KO+EtOH
Gabra1fl/fl+GABA+EtOH
Gabra1IEC-KO+GABA+EtOH
H&E
200 μm
50 μm
E
ALT (U/L)
ns
**
F
Oil red O
G
Hepatic TG (mmol/gprot)
*
H
I
Occludin
59 kDa
Claudin 1
22 kDa
Claudin 4
22 kDa
β-actin
43 kDa

Figure 8. Intestinal epithelial-specific Gabra1 gene knockout confers protection in ALD mice.

(A) AAV9-villin-cre virus or AAV9-villin-NC virus were injected into Gabra1fl/fl mice for 3 weeks to construct an intestinal epithelial cell-specific Gabra1 knockout (Gabra1IEC-KO) or negative control mouse model. Subsequently, Gao-binge ethanol treatment and/or GABA (daily i.p. 200 mg/kg) were administered to the indicated group. (B) Organ-specific detection of AAV9-villin-cre virus transfection, with green fluorescence representing the virus. (C) Western blot analysis used to assess the efficiency of intestinal epithelial-specific Gabra1 gene knockout. (D) Histological examination of mouse liver tissues via H&E staining revealed increased lipid vacuoles in the Gabra1IEC-KO mice. (E) Determination of serum ALT levels (n=4/group). (F) Oil Red O staining of mouse liver tissues. (G) Hepatic TG levels (n=4/group). (H) Lactobacillus cultures were used to detect colony formation in liver homogenates. (I) Western blot analysis of the expression of colonic tight junction proteins in mice. Significance levels denoted as *P < 0.05, **P < 0.01, ***P < 0.001, ns, not statistically significant.

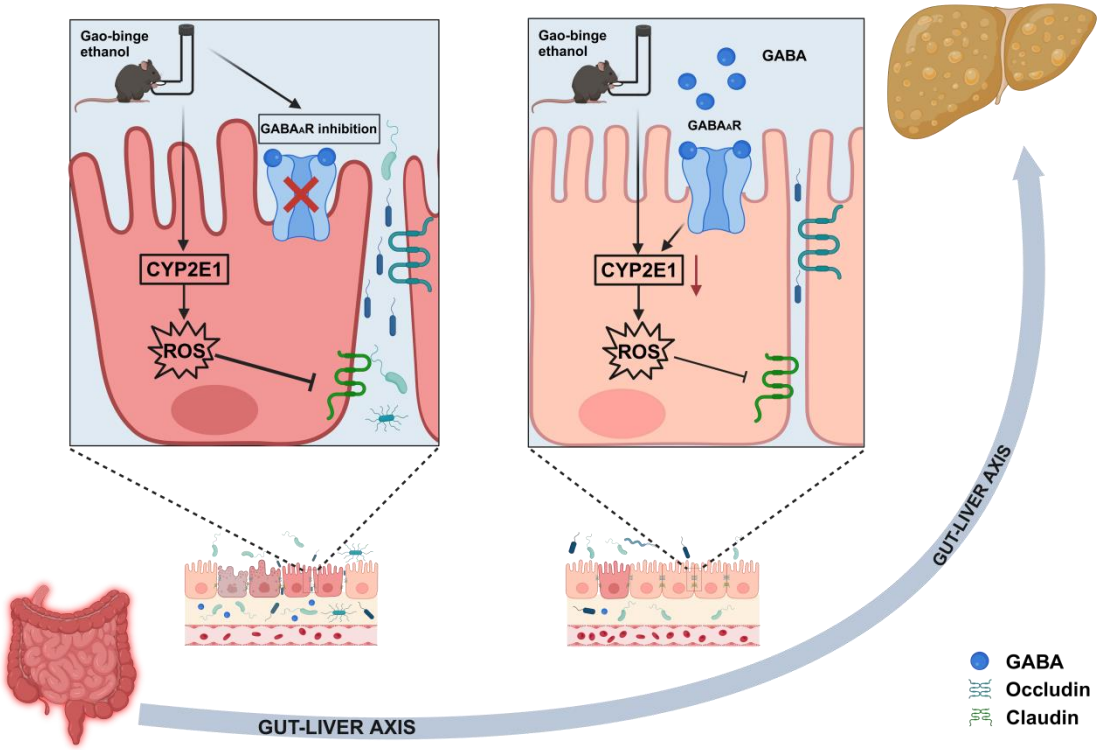

Figure 9. Summary diagram of the intestinal epithelial GABA signaling mechanisms involved in regulating ALD progression.

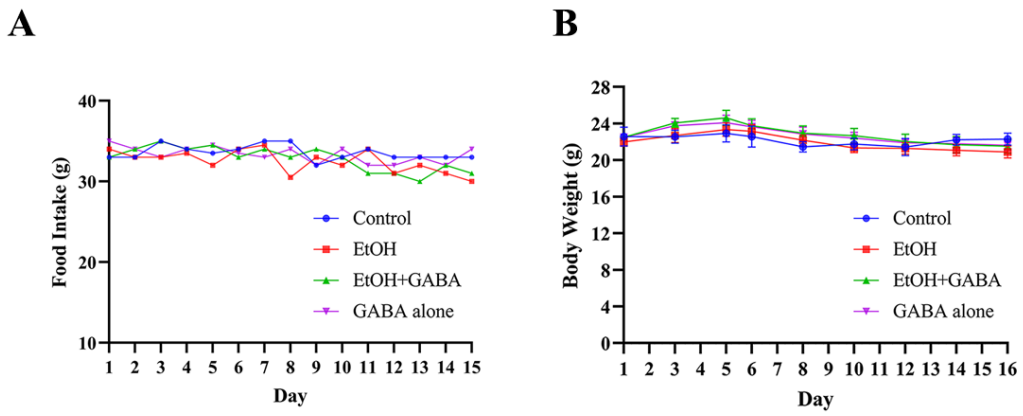

Supplementary Figure 1. Group-wise Analysis of Food Intake and Body Weight in a Gao-binge Mouse Model of Alcohol-associated Liver Disease.

(A) Food intake and (B) body weight of mice within each group during generation of the model.

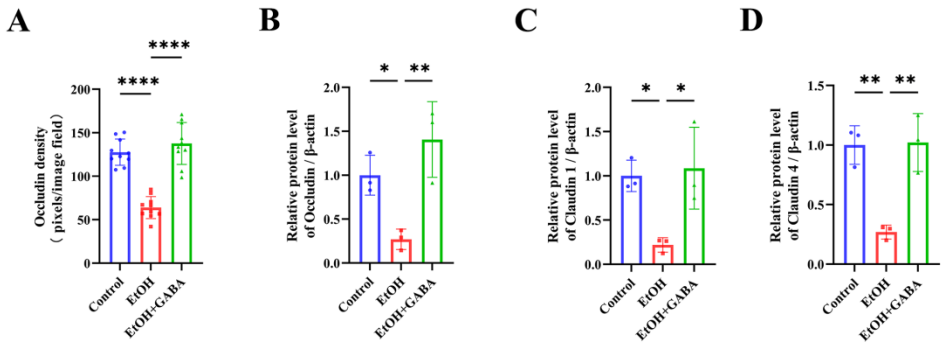

Supplementary Figure 2. Expression Analysis of Tight Junction Proteins in Murine Colon in Gao-binge ALD mice.

(A) Quantitative analysis of Occludin immunofluorescence intensity in mouse colon tissues (n=6/group). (B-D) Quantification of protein expression levels of Occludin, Claudin 1 and Claudin 4 as normalized to β-actin (n=3/group). Significance levels denoted as $*P < 0.05$, $***P < 0.001$, $****P < 0.0001$, ns, not statistically significant.

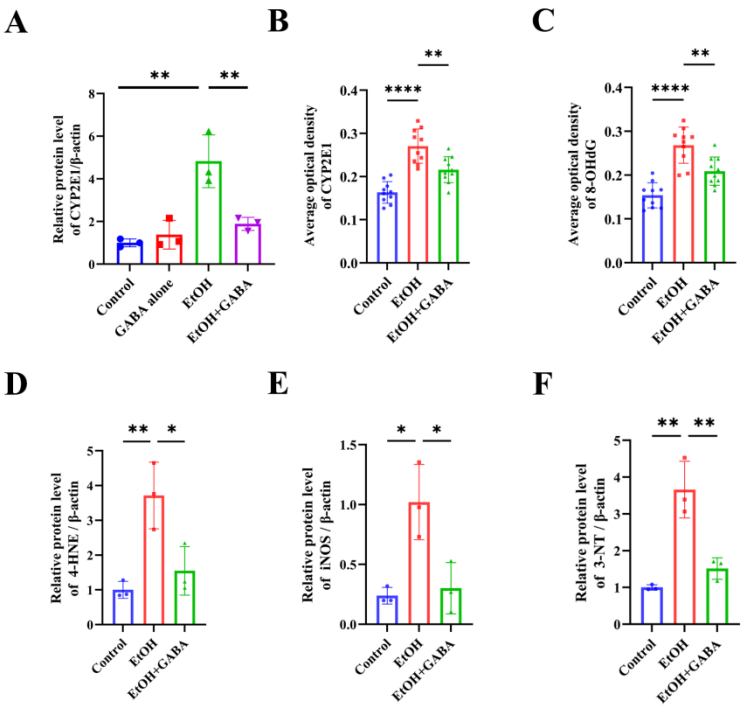

Supplementary Figure 3. Quantitative Profiling of Oxidative Stress and Injury Markers in the Colon.

(A) Quantification of CYP2E1 protein expression levels as normalized to β-actin (n=3/group). (B) Quantitative analysis of CYP2E1-positive area in mouse colon sections (n=6/group). (C) Quantitative analysis of 8-OHdG-positive area in mouse colon sections (n=6/group). (D-F) Quantification of 4-HNE, iNOS and 3-NT protein expression levels as normalized to β-actin (n=3/group). Significance levels denoted as ****$P < 0.0001$, ns, not statistically significant.

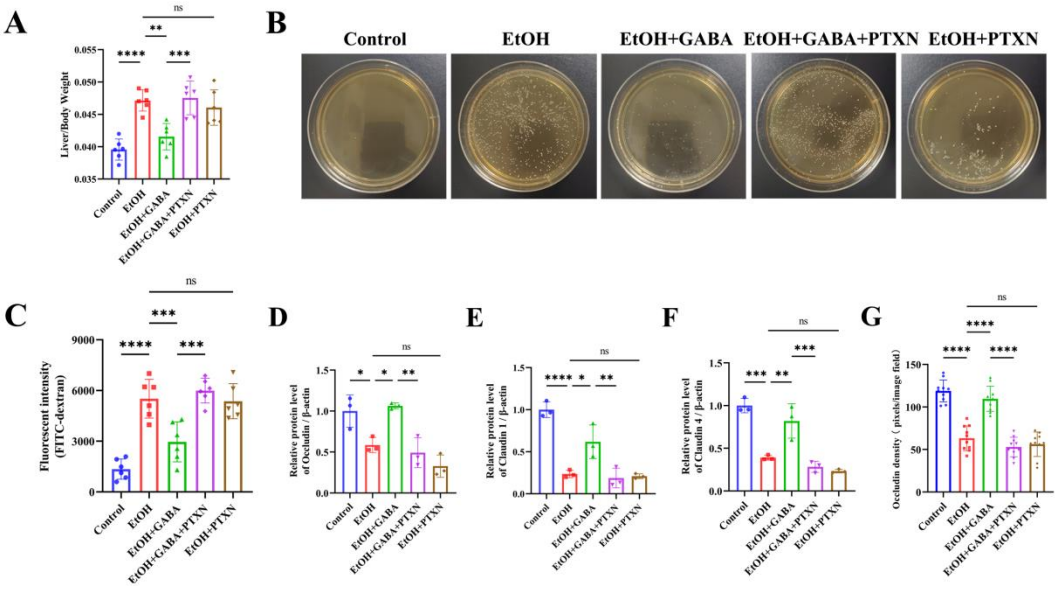

Supplementary Figure 4. Comprehensive Assessment of Gut-Liver Axis Function and Intestinal Barrier Integrity.

(A)Comparative analysis of liver index within the different groups (n=6/group). (B) Lactobacillus cultures were used to detect colony formation in liver homogenates. (C) Intestinal permeability as assessed with use of the fluorescein isothiocyanate FITC‑dextran test (n=6/group). (D-F) Quantification of Occludin, Claudin 1, and Claudin 4 protein expression levels as normalized to β-actin (n=3/group). (G) Quantitative analysis of Occludin immunofluorescence intensity in mouse colon sections (n=10/group). Significance levels denoted as $*P < 0.05$, $**P < 0.01$, ns, not statistically significant.

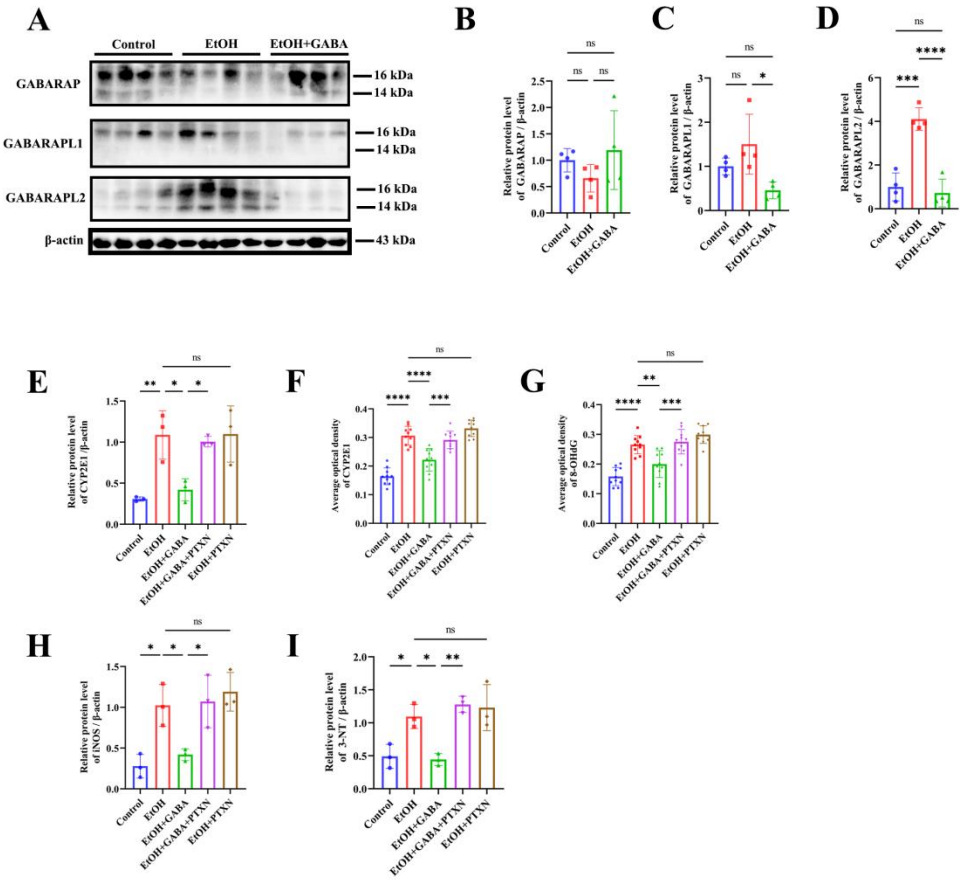

Supplementary Figure 5. Expression Profiling of GABA Receptor-Associated Proteins and Oxidative Stress Markers in the Murine Colon.

(A) Western blot analysis of the expression of colonic GABARAP, GABARAPL1, GABARAPL2 in mice. (B) Quantification of GABARAP protein expression levels as normalized to β-actin (n=3/group). (C) Quantification of GABARAPL1 protein expression levels as normalized to β-actin (n=3/group). (D) Quantification of GABARAPL2 protein expression levels as normalized to β-actin. (E)Western blot analysis of the expression of colonic CYP2E1 in mice. (F) Quantification of CYP2E1 protein expression levels as normalized to β-actin (n=3/group). (G) Quantitative analysis of 8-OHdG-positive area in mouse colon sections (n=6/group). (H-I) Quantification of iNOS and 3-NT protein expression levels as normalized to β-actin (n=3/group). Significance levels denoted as $*P < 0.05$, $**P < 0.01$, $***P < 0.001$, $****P < 0.0001$, ns, not statistically significant.

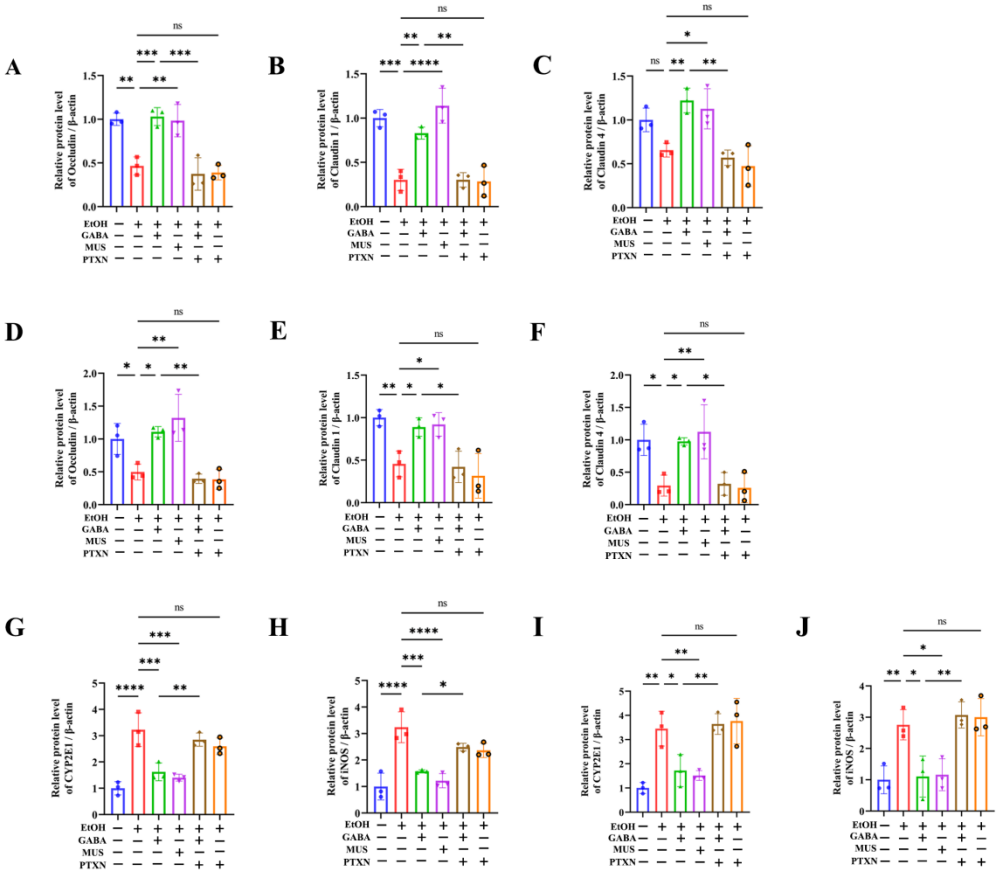

Supplementary Figure 6. Analysis of Tight Junction Protein and Metabolic Enzyme Expression in Colonic Epithelial Cell Lines

(A-C) Quantitative analysis of Occludin, Claudin 1, and Claudin 4 protein expression levels in CCD841 cells as normalized to β-actin (n=3/group). (D-F) Quantitative analysis of Occludin, Claudin 1, and Claudin 4 protein expression levels in T84 cells as normalized to β-actin. (n=3/group). (G-H) Quantitative analysis of CYP2E1 and iNOS protein expression levels in CCD841 cells as normalized to β-actin. (n=3/group). (I-J) Quantitative analysis of CYP2E1 and iNOS protein expression levels in T84 cells as normalized to β-actin (n=3/group). Significance levels denoted as $*P < 0.05$, $**P < 0.01$, $***P < 0.001$, $****P < 0.0001$, ns, not statistically significant.

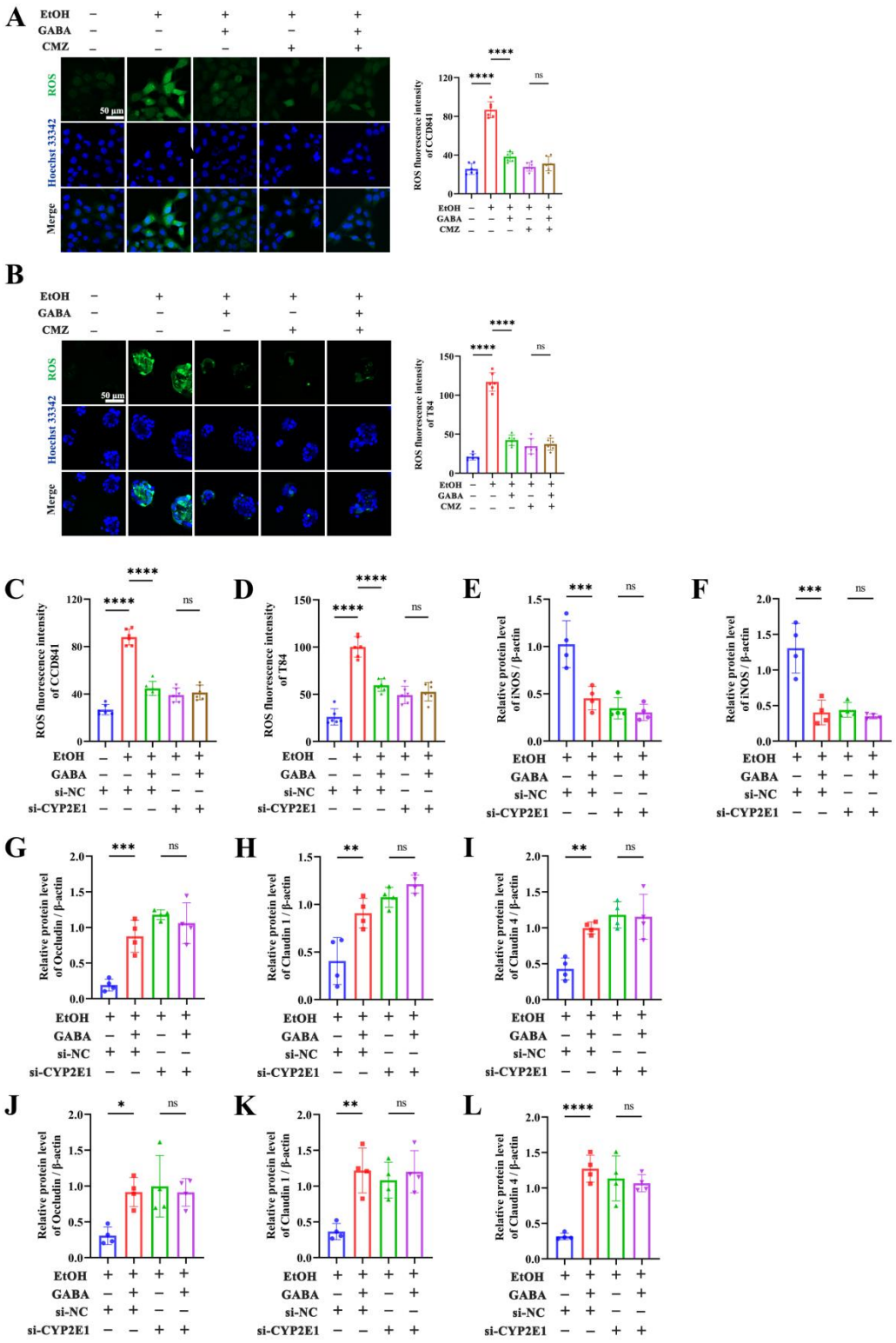

Supplementary Figure 7. Modulation of ethanol-induced oxidative stress and barrier protein expression by GABA and CYP2E1 inhibition in colonic epithelial cells

(A) Fluorescent detection and quantitative analysis of ROS in ethanol-challenged CCD841 cells treated with GABA (50 μM) or the CYP2E1 inhibitor, Clomethiazole (CMZ, 50 μM) (n=3/group). (B) Fluorescence detection and quantitative analysis of ROS in ethanol-challenged T84 cells treated with GABA (50 μM) and CMZ (50 μM) (n=3/group). (C-D) Quantitative analysis of ROS levels in ethanol-challenged CCD841 (C) and T84 (D) cells transfected with si-CYP2E1 or siRNA negative control (n=6/group). (E) Quantitative analysis of iNOS protein expression levels in CCD841 cells as normalized to β-actin (n=4/group). (F) Quantitative analysis of iNOS protein expression levels in T84 cells as normalized to β-actin (n=4/group).

(G-I) Quantitative analysis of Occludin, Claudin 1, and Claudin 4 protein expression levels in CCD841 cells as normalized to β-actin (n=4/group). (J-L) Quantitative analysis of Occludin, Claudin 1, and Claudin 4 protein expression levels in T84 cells as normalized to β-actin (n=4/group). Significance levels denoted as $*P < 0.05$, $**P < 0.01$, $***P < 0.001$, $****P < 0.0001$, ns, not statistically significant.

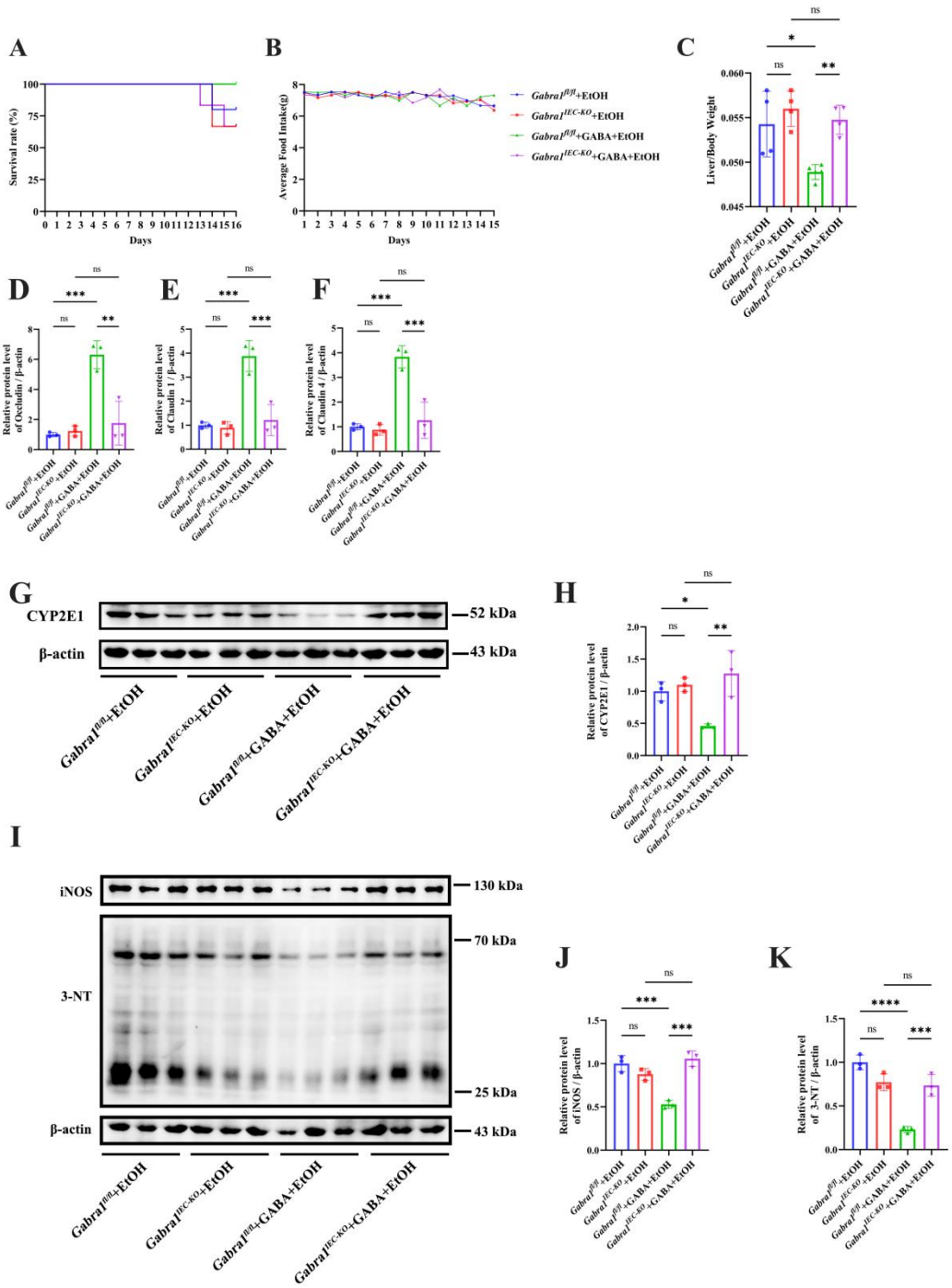

Supplementary Figure 8. Effects of GABRA1 Knockout on Survival, Hepatic Index, and Intestinal Barrier and Stress Protein Expression in a Mouse Model of ALD

(A) Statistical analysis of survival rates in each group of mice during modeling. (B) Changes in average food intake in each group of mice during modeling. (C) Comparison of liver indices among the different groups of mice (n=4/group). (D-F) Quantification of Occludin, Claudin 1, and Claudin 4 protein expression levels as normalized to β-actin (n=3/group). (G) Western blot analysis of the expression of

colonic CYP2E1 in mice. (H) Quantification of CYP2E1 protein expression levels as normalized to β-actin (n=3/group). (I) Western blot analysis of intestinal expressions of iNOS and 3-NT. (J-K) Quantification of iNOS and 3-NT protein expression levels as normalized to β-actin (n=3/group). Significance levels denoted as *P < 0.05, **P < 0.01, ***P < 0.001, ****P < 0.0001, ns, not statistically significant.

[1] PANDE A, SHARMA S, KHILLAN V, RASTOGI A, ARORA V, SHASTHRY S M, VIJAYARAGHAVAN R, JAGDISH R, KUMAR M, KUMAR G, MONDOT S, DORE J, SARIN S K. Fecal microbiota transplantation compared with prednisolone in severe alcoholic hepatitis patients: a randomized trial [J]. Hepatol Int, 2023, 17(1): 249-61.

[2] VATSALYA V, FENG W, KONG M, HU H, SZABO G, MCCULLOUGH A, DASARATHY S, NAGY L E, RADAEVA S, BARTON B, MITCHELL M, MCCLAIN C J. The Beneficial Effects of Lactobacillus GG Therapy on Liver and Drinking Assessments in Patients with Moderate Alcohol-Associated Hepatitis [J]. Am J Gastroenterol, 2023, 118(8): 1457-60.

[3] SUH G A. Phage Therapy for Alcohol-Associated Hepatitis [J]. Hepatology, 2021, 73(4): 1609-10.

[4] BEN-SHAANAN T L, SCHILLER M, AZULAY-DEBBY H, KORIN B, BOSHNAK N, KOREN T, KROT M, SHAKYA J, RAHAT M A, HAKIM F, ROLLS A. Modulation of anti-tumor immunity by the brain's reward system [J]. Nat Commun, 2018, 9(1): 2723.

[5] BAO Z, CHEN X, LI Y, JIANG W, PAN D, MA L, WU Y, CHEN Y, CHEN C, WANG L, ZHAO S, WANG T, LU W Y, MA C, WANG S. The hepatic GABAergic system promotes liver macrophage M2 polarization and mediates HBV replication in mice [J]. Antiviral Res, 2023, 217: 105680.

[6] DENG Z, LI D, WANG L, LAN J, WANG J, MA Y. Activation of GABA(B)R Attenuates Intestinal Inflammation by Reducing Oxidative Stress through Modulating the TLR4/MyD88/NLRP3 Pathway and Gut Microbiota Abundance [J]. Antioxidants (Basel), 2024, 13(9).

[7] TENG J, YU T, YAN F. GABA attenuates neurotoxicity of zinc oxide nanoparticles due to oxidative stress via DAF-16/FoxO and SKN-1/Nrf2 pathways [J]. Sci Total Environ, 2024, 934: 173214.